Published ind: Nature metabolism (2021), vol. 3, n°10, pp. 1342-1356
DOI: 10.1038/s42255-021-00469-6
Status : Postprint (Author's version)

FASTING-MIMICKING DIET PREVENTS HIGH-FAT DIET EFFECT ON CARDIOMETABOLIC RISK AND LIFESPAN

Amrendra Mishra[1*], Hamed Mirzaei[1*], Novella Guidi[1*], Manlio Vinciguerra[2], Alice Mouton[3], Marina Linardic[4], Francesca Rappa[5], Rosario Barone[5], Gerardo Navarrete[1], Min Wei[1], Sebastian Brandhorst[1], Stefano Di Biase[1], Todd E. Morgan[1], S. Ram Kumar[6], Peter S. Conti[7], Matteo Pellegrini[4], Michel Bernier[8], Rafael de Cabo[8] and Valter D. Longo[1, 9]

[1]*Longevity Institute and Davis School of Gerontology, University of Southern California, Los Angeles, CA, USA.*
[2]*International Clinical Research Center, St Anne's University Hospital, Brno, Czech Republic*
[3]*Department of Ecology and Evolutionary Biology, University of California, Los Angeles, CA, USA.*
[4]*Department of Molecular, Cell and Developmental Biology, University of California, Los Angeles, CA, USA.*
[5]*Section of Human Anatomy, Department of Biomedicine, Neuroscience and Advanced Diagnostics (BIND), University of Palermo, Palermo, Italy*
[6]*Department of Surgery, Keck School of Medicine, University of Southern California, Los Angeles, CA, USA.*
[7]*Molecular Imaging Center, Department of Radiology, Keck School of Medicine, University of Southern California, Los Angeles, CA, USA.*
[8]*Translational Gerontology Branch, Intramural Research Program of the National Institute on Aging, National Institutes of Health, Baltimore, MD, USA.*
[9]*IFOM, FIRC Institute of Molecular Oncology, Milano, Italy.*

**These authors contributed equally: Amrendra Mishra, Hamed Mirzaei, Novella Guidi.* ✉ *e-mail: vlongo@usc.edu*

ABSTRACT

Diet-induced obesity is a major risk factor for metabolic syndrome, diabetes and cardiovascular disease. Here, we show that a 5-d fasting-mimicking diet (FMD), administered every 4 weeks for a period of 2 years, ameliorates the detrimental changes caused by consumption of a high-fat, high-calorie diet (HFCD) in female mice. We demonstrate that monthly FMD cycles inhibit HFCD-mediated obesity by reducing the accumulation of visceral and subcutaneous fat without causing loss of lean body mass. FMD cycles increase cardiac vascularity and function and resistance to cardiotoxins, prevent HFCD-dependent hyperglycaemia, hypercholesterolaemia and hyperleptinaemia and ameliorate impaired glucose and insulin tolerance. The effect of monthly FMD cycles on gene expression associated with mitochondrial metabolism and biogenesis in adipocytes and the sustained ketogenesis in HFCD-fed mice indicate a role for fat cell reprogramming in obesity prevention. These effects of an FMD on adiposity and cardiac ageing could explain the protection from HFCD-dependent early mortality.

The National Health and Nutrition Examination Survey 2020 concluded that 42.4% of adults in the

USA were obese in 2017-2018, up from 39.8% in 2016-2017 and 15.0% for the period of 1976-1980 (refs.[1,2]). A high-calorie diet combined with a sedentary lifestyle is the major cause of obesity[3], a central risk factor associated with the development of metabolic syndrome and cardiovascular disease (CVD)[4].

Multiple human studies have found a correlation between the fat content of diet and the incidence of obesity, indicating that a high-fat diet (HFD) combined with 'standard' levels of carbohydrates and proteins is sufficient to promote obesity[3,5]. Rodent models of diet-induced obesity (DIO), which have shed light on the mechanisms underlying metabolic syndrome, CVD and diabetes[6], also indicate that the consumption of food high in fat but not in protein or sucrose increases adiposity[7].

Different dietary interventions that involve periods of fasting are potentially beneficial for the treatment of obesity, metabolic syndrome and CVD as well as slowing down the ageing process[8,9]. In previous studies, we developed a hypocaloric FMD that contained high levels of dietary fat but low levels of protein and carbohydrate and reported that short periodic treatment with the FMD provides benefits similar to chronic calorie restriction without the risk of malnutrition[10]. The initial study reported that FMD administered to mice for 4 d twice a month resulted in health benefits and physiological changes comparable to those observed after continuous calorie restriction but without side effects including muscle or bone density loss[10]. Periodic FMD cycles lasting 2-5 d cause a range of health benefits, including increased longevity, a decrease and delay in cancer incidence, reduced autoimmunity and multiple sclerosis symptoms, reversal of type 1 and type 2 diabetes pathology, modulation of gut microbiota and intestinal regeneration, and reversal of inflammatory bowel disease pathology[9-14].

In the current study, we focused on exploring the effect of less-frequent monthly 5-d FMD cycles on a mouse model of DIO and metabolic syndrome. Specifically, we tested whether periodic FMD cycles can reverse the effects of an HFCD on survival, body weight and cardiac ageing as well as several circulating metabolic parameters. We also explored the molecular changes induced by the HFCD and affected by cycles of the FMD by transcriptome sequencing of visceral adipose tissue (VAT) and heart tissue.

Results

Periodic FMD prevents HFCD-induced obesity and early mortality. To test the effects of periodic FMD in a mouse model of DIO, 9-11-month-old female C57BL/6 mice were fed ad libitum either a control diet (10% calories from fat), a commercial HFCD (60% calories from fat) or an HFCD combined once every 4 weeks with a 5-d cycle of the FMD (HFCD + FMD). As female C57BL/6J mice are less susceptible to DIO and pathology than their male counterparts[15], we used an HFD (60%) instead of a more moderate fat (45%) diet. All other components of the diet were matched in the HFCD and control diet including sucrose (Supplementary Table 1). Mice usually consumed all of the day 1 FMD but often did not eat part of the day 2-5 FMD (providing 10% of normal calorie intake). During the first five cycles of the FMD, the abrupt change from the FMD (near-fasting condition) to the high-calorie HFCD was not well tolerated by mice; therefore, starting at cycle 6, the 5-d FMD period was followed by 2 d of a control diet with normal calorie levels before switching to the HFCD (outlined in Fig. 1a and Extended Data Fig. 1). The HFCD led to the development of obesity in mice continuously fed the obesogenic diet, whereas mice undergoing cycles of the FMD (HFCD + FMD

group) did not develop obesity and had a body weight similar to that of mice fed the control diet (Fig. 1b,f).

Figure 1 - The FMD increases longevity and limits body fat accumulation and weight gain. ***a****, Schematic representation of diet regimens and intervals of the FMD. The FMD diet consists of 5 d per month cycle during which mice are fed 50% of the normal daily calorie intake on day 1 and 10% of the normal daily calorie intake on days 2-5. Female C57BL6 mice (9-11 months old) were divided into three groups (n = 46-49 per group) based on the following regimen: control diet (CD), HFCD and HFCD followed by cycles of FMD (HFCD + FMD). Mice were fed their respective diets either for the whole lifespan period (for the longevity study) or until they were used for different analyses.* ***b****, Representative pictures of mice on different diet regimens 5 d after completion of cycle 18 of the FMD.* ***c****, Kaplan-Meier survival curve of mice on control, HFCD and HFCD + FMD diets. Log-rank (Mantel-Cox) test, control versus HFCD, ****P < 0.0001; control versus HFCD + FMD, P = 0.0630 (NS); HFCD versus HFCD + FMD, ***P = 0.0005. Median survival, control, 836.5 d; HFCD, 570 d; HFCD + FMD, 732 d; control (n = 46), HFCD (n = 49), HFCD + FMD (n = 46).* ***d****, Body weight trajectories after ten cycles of the FMD. Data are shown as mean ± s.e.m. One-way ANOVA, P < 0.0001, Tukey's multiple-comparisons tests, control versus HFCD, ****P < 0.0001; control versus HFCD + FMD, ****P < 0.0001; HFCD versus HFCD + FMD, ****P < 0.0001. n = 29-58 mice per group. Dashed vertical lines denote the FMD cycle.* ***e****, Percent body weight (BW) changes from baseline after ten cycles of the FMD. Body weight was measured 1 week after the FMD. One-way ANOVA, P value < 0.0001. Control (n = 44), HFCD (n = 28), HFCD + FMD (n = 43).* ***f****, Body weight after 18 cycles of the FMD (13 d after the end of the FMD). One-way ANOVA, ****P < 0.0001, Tukey's multiple-comparisons tests, control versus HFCD, ****P < 0.0001; control versus HFCD + FMD, ****P < 0.0001; HFCD versus HFCD + FMD, ****P < 0.0001. Control (n = 7), HFCD (n = 12), HFCD + FMD (n = 16).* ***g****, Volume of VAT and SAT and percent VAT/SAT measured by MRI after 22 cycles of the FMD (2 weeks after the end of the FMD). SAT, one-way ANOVA, ***P = 0.0004, Tukey's multiple-comparisons tests, control versus HFCD, ***P = 0.0006; control versus HFCD + FMD, P = 0.8670 (NS); HFCD versus HFCD + FMD, **P = 0.0014. VAT, one-way ANOVA, ***P = 0.0006, Tukey's multiple-comparisons tests, control versus HFCD, **P = 0.0012; control versus HFCD + FMD, P = 0.9844 (NS); HFCD versus HFCD + FMD, **P = 0.0015. Percent VAT/SAT, one-way ANOVA, P value = 0.0345, Tukey's multiple-comparisons tests, control versus HFCD, P = 0.1772 (NS); control versus HFCD + FMD, P = 0.5616 (NS); HFCD versus HFCD + FMD, *P = 0.0296. n = 5 per group.* ***h****, Representative MRI scans demonstrate changes in body fat composition for each group. All data are shown as mean ± s.e.m.*

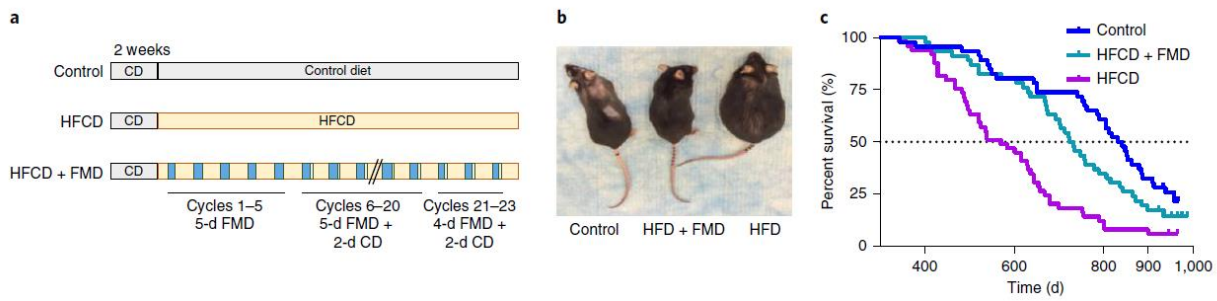

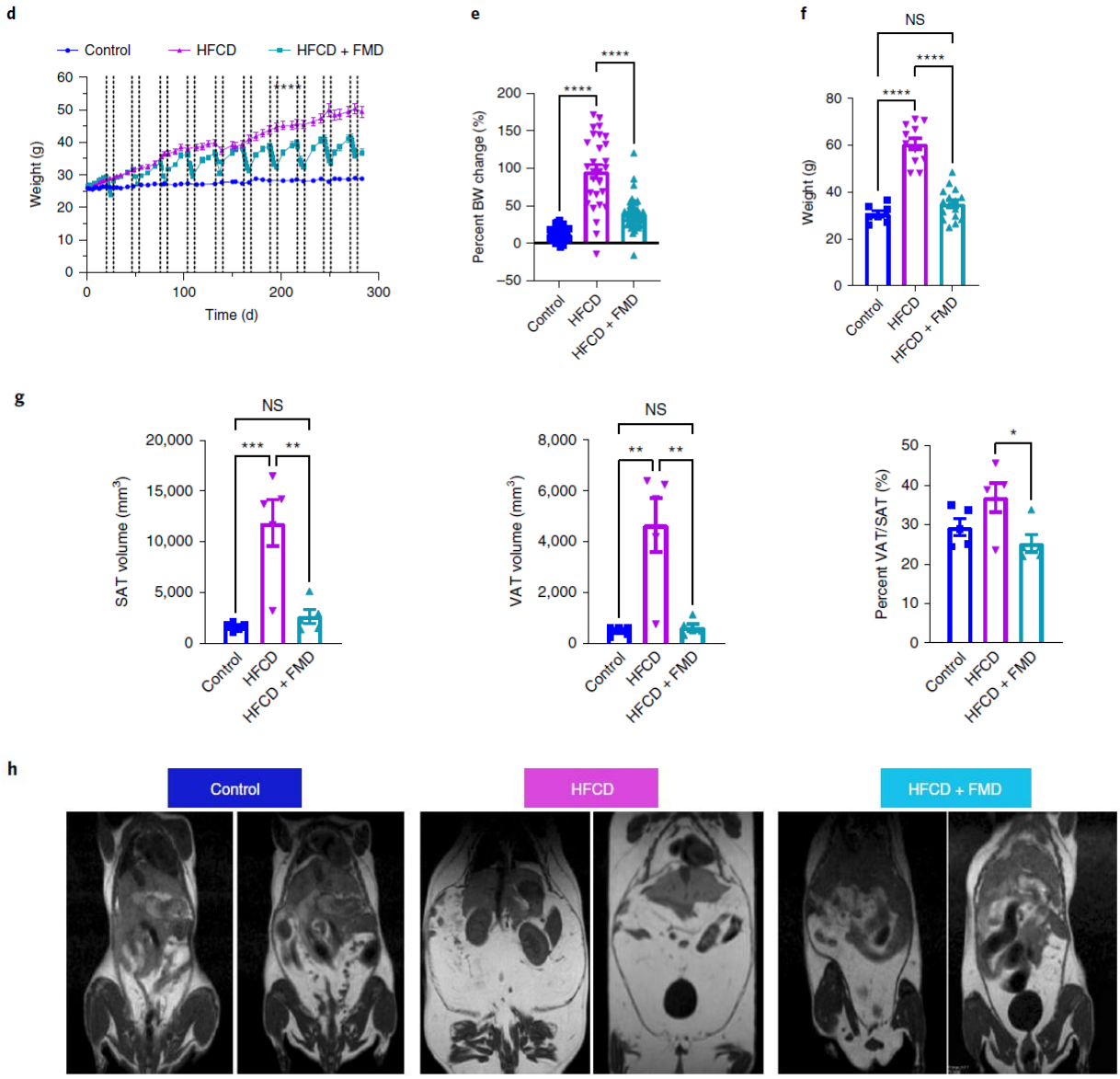

Mice fed an HFCD also showed a reduced median survival compared to mice on the control diet, an effect that was largely rescued by periodic FMD cycles (HFCD + FMD, median survival; control = 836.5 d, HFCD = 570 d, HFCD + FMD = 732 d, log-rank (Mantel-Cox) test *P* value < 0.0001, control versus HFCD, *P* value < 0.0001; control versus HFCD + FMD, *P* value = 0.0630 (not significant (NS)); HFCD versus HFCD + FMD, *P* value = 0.0005) (Fig. 1c). Mice in all groups gained weight over time with the biggest gain occurring in the HFCD group (Fig. 1d). Control, HFCD and HFCD + FMD groups gained 12.02%, 95.45% and 38.80% of body weight, respectively, over a 10-month period (ten cycles of the FMD, Fig. 1e). With age, HFCD-fed mice gained weight faster than mice on the HFCD + FMD regimen, although both groups had similar body weight until approximately day 100 (on the diet), when the weight of both groups began to separate (Fig. 1d). Mean body weights of control, HFCD-fed and HFCD + FMD-fed mice after 18 months on their respective diets (2 weeks after the end of the FMD cycle) were 30.73 g, 60.63 g and 34.88 g, respectively, with the HFCD + FMD group showing weight only 13.5% higher than that of the control group (Fig. 1f, one-way ANOVA, *P* value < 0.0001; Tukey's multiple-comparisons test, control versus HFCD + FMD, *P* = 0.3826 (NS); control versus HFCD, *P* < 0.0001; HFCD + FMD versus HFCD, *P* < 0.0001). By contrast, the weight gain of the

HFCD group was 97.29% over that of the control, similar to the result at 10 months (Fig. 1e,f).

Magnetic resonance imaging (MRI) scans were performed to quantify the body fat content of mice on different diet regimens. The HFCD led to a significant accumulation of both visceral and subcutaneous fat as compared to the control diet and HFCD + FMD; mice in the latter two groups showed similar body fat composition (Fig. 1g,h). Mice on the HFCD + FMD also displayed a lower percent of VAT to subcutaneous adipose tissue (SAT) (percent VAT/ SAT) than mice on either the HFCD or the control diet (Fig. 1g,h, one-way ANOVA, *P* value = 0.0345). In summary, cycles of a 5-d FMD once every 4 weeks followed by 2 d of control diet were able to prevent the effects of the HFCD on lifespan and adiposity.

Figure 2 | *FMD cycles improve health biomarkers in HFCD-fed mice.* ***a****, Measurement of body composition by quantification of body weight, fat mass, lean body mass and fluid content by nuclear magnetic resonance at the end of 13 cycles, 17 d after the end of the FMD. Fat, one-way ANOVA, ****P < 0.0001, Tukey's multiple-comparisons tests, control versus HFCD, ****P < 0.0001; control versus HFCD + FMD, P = 0.2873 (NS); HFCD versus HFCD + FMD, ****P < 0.0001. Fluid, one-way ANOVA, ****P < 0.0001; Tukey's multiple-comparisons tests, control versus HFCD, ****P < 0.0001; control versus HFCD + FMD, P = 0.0524 (NS); HFCD versus HFCD + FMD, ****P < 0.0001. Lean mass, one-way ANOVA, P value = 0.2672 (NS), Tukey's multiple-comparisons tests, control versus HFCD, P = 0.2692 (NS); control versus HFCD + FMD, P = 0.3474 (NS); HFCD versus HFCD + FMD, P = 0.9775 (NS). Control (n = 6), HFCD (n = 11), HFCD + FMD (n = 11).* ***b****, Serum cholesterol levels measured at different time points over the course of study, measured 4 d after refeeding. One-way ANOVA, ****P < 0.0001, Tukey's multiple-comparisons tests, eight cycles, control versus HFCD (*P = 0.0167), control versus HFCD + FMD (P = 0.7008 (NS)), HFCD versus HFCD + FMD (P = 0.8855 (NS)); 23 cycles, control versus HFCD (****P < 0.0001), control versus HFCD + FMD (P = 0.7385 (NS)), HFCD versus HFCD + FMD (****P < 0.0001). Baseline (n = 6); four cycles, control (n = 8), HFCD (n = 8), HFCD + FMD (n = 8); eight cycles, control (n = 8), HFCD (n = 16), HFCD + FMD (n = 8); 23 cycles, control (n = 11), HFCD (n = 5), HFCD + FMD (n = 7).* ***c****, Serum triglyceride levels measured after eight cycles (11 d after the FMD) and 14 cycles (18 d after the FMD) of the FMD. Two-way ANOVA, P = 0.5003, Tukey's multiple-comparisons tests, eight cycles, control versus HFCD (P = 0.8358 (NS)), control versus HFCD + FMD (P = 0.9104 (NS)), HFCD versus HFCD + FMD (P = 0.6385 (NS)); 14 cycles, control versus HFCD (P = 0.7596 (NS)), control versus HFCD + FMD (P = 0.9999 (NS)), HFCD versus HFCD + FMD (P = 0.7491). Eight cycles, control (n = 8), HFCD (n = 4), HFCD + FMD (n = 8); 14 cycles, control (n = 5), HFCD (n = 5), HFCD + FMD (n = 6).* ***d****, Serum ketone body levels measured at the end of four cycles of the FMD, 4 d after refeeding. One-way ANOVA, *P = 0.0108, Tukey's multiple-comparisons tests, control versus HFCD, P = 0.9954 (NS); control versus HFCD + FMD, *P = 0.0161; HFCD versus HFCD + FMD, *P = 0.0278. Baseline (n = 6), control (n = 8), HFCD (n = 8), HFCD + FMD (n = 8).* ***e****, Serum leptin levels measured after eight cycles of the FMD, 11 d after refeeding. One-way ANOVA, ****P < 0.0001, Tukey's multiple-comparisons tests, control versus HFCD, ****P < 0.0001; control versus HFCD + FMD, P = 0.3963 (NS); HFCD versus HFCD + FMD, ****P < 0.0001. Control (n = 7), HFCD (n = 4), HFCD + FMD (n = 8).* ***f****, Serum ghrelin levels measured after eight cycles of the FMD, 11 d after refeeding. One-way ANOVA, P = 0.0551. Control (n = 6), HFCD (n = 2), HFCD + FMD (n = 6).* ***g****, Blood glucose levels measured at baseline and after five cycles of the FMD, 2 d after refeeding. Two-way ANOVA, P < 0.0001, Tukey's multiple-comparisons tests, baseline, control versus HFCD (P = 0.9954), control versus HFCD + FMD (P = 0.5154 (NS)), HFCD versus HFCD + FMD (P = 0.4782 (NS)); five cycles, control versus HFCD (****P < 0.0001), control versus HFCD + FMD (P = 0.0549 (NS)), HFCD versus HFCD + FMD (****P < 0.0001). Baseline, control (n = 10), HFCD (n = 9), HFCD + FMD (n = 10); five cycles, control (n = 10), HFCD (n = 9), HFCD + FMD (n = 10).* ***h****,****i****, GTT after five cycles of the FMD, 2 d after the end of the FMD.* ***h****, Blood glucose levels following oral glucose gavage during a time course of 120 min.* ***i****, AUC of glucose levels in different groups during the 120-min GTT. One-way ANOVA, *P = 0.0190, Tukey's multiple-comparisons tests, control versus HFCD, P = 0.3298 (NS); control*

*versus HFCD + FMD, P = 0.1945 (NS); HFCD versus HFCD + FMD, *P = 0.0150. n = 5 per group.* ***j,k****, ITT following four cycles of the FMD, 2 d after the FMD.* ***j****, Blood glucose levels following intraperitoneal injection of insulin during the time course of 120 min.* ***k****, AUC of glucose levels in different groups during the 120-min ITT. One-way ANOVA, **P = 0.0011, Tukey's multiple-comparisons tests, control versus HFCD, *P = 0.0422; control versus HFCD + FMD, P = 0.0990 (NS); HFCD versus HFCD + FMD, ***P = 0.0008. n = 5 per group. All data are shown as mean ± s.e.m.*

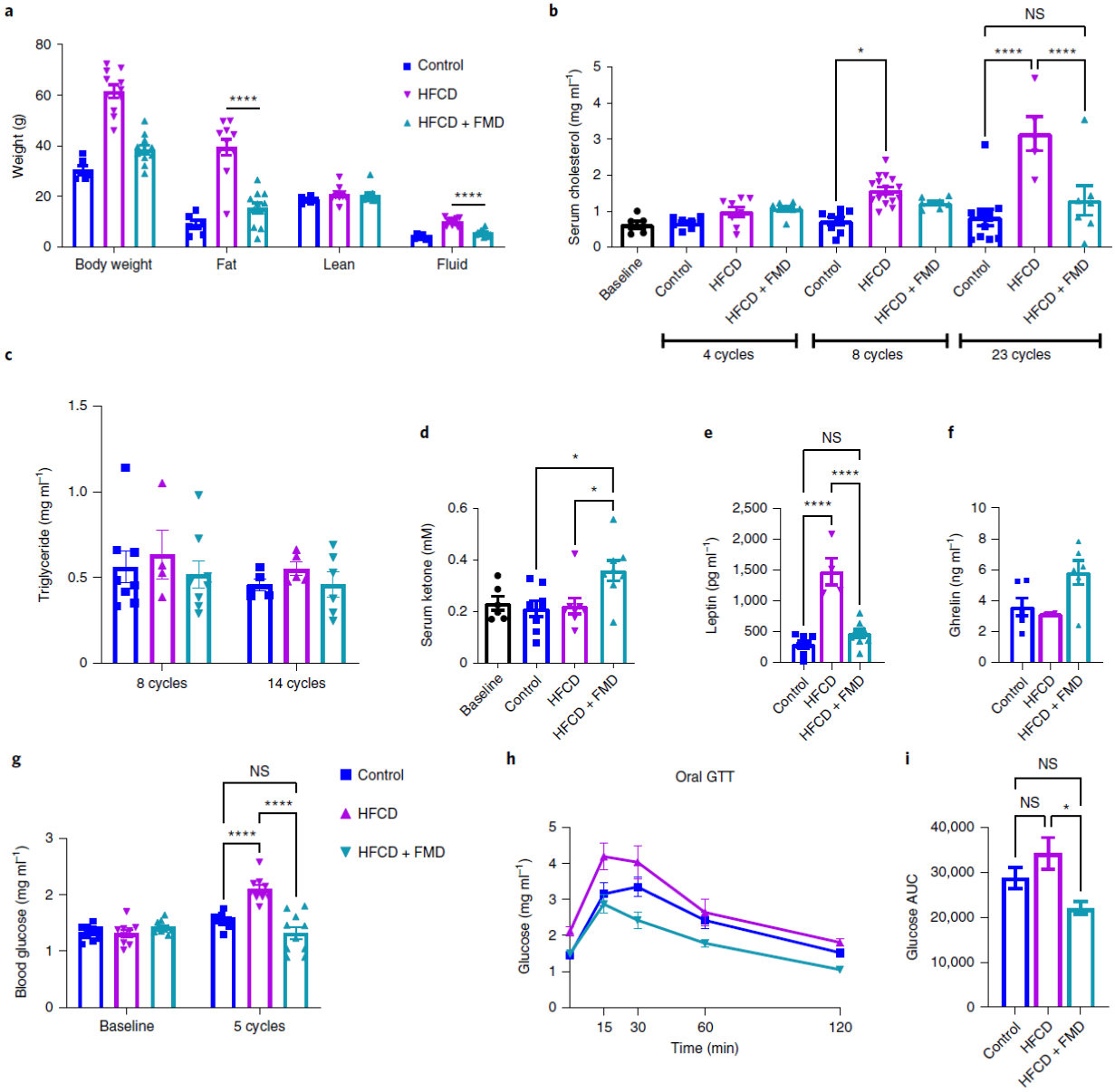

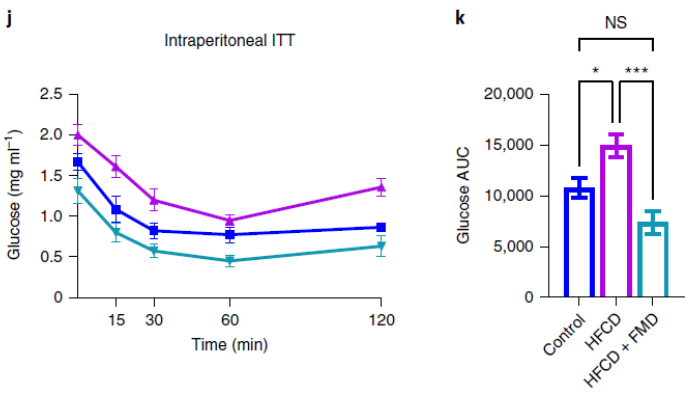

Figure 3 - FMD cycles rewire metabolism for preferential utilization of fat, lowering calorie intake in HFCD-fed mice. ***a****, Outline of the experiment. Female C57BL/6 mice (4-6 months old) underwent two cycles of the FMD, and measurements were taken inside the metabolic cage beginning 3 d before the start of the FMD cycle and until 10 d after the end of the FMD cycle. Each monthly FMD cycle consisted of a 4-d FMD followed by the control diet for 2 d before switching to the HFCD diet.* ***b****, Cumulative food intake (kcal) per mouse in a representative FMD cycle (14-d period) in each group. n = 4 mice per group. One-way ANOVA, ***P = 0.0002. Tukey's multiple-comparisons tests, control versus control with FMD, P = 0.5430 (NS); control versus HFCD, **P = 0.0079; control versus HFCD + FMD, P = 0.3924 (NS); control with FMD versus HFCD, ***P = 0.0005; control with FMD versus HFCD + FMD, P = 0.9895 (NS); HFCD versus HFCD + FMD, ***P = 0.0003.* ***c****,****d****, Average percent body weight change on each day.* ***e****,****f****, Cumulative food intake (kcal) per mouse.* ***g****,****h****, RER (VCO_2/VO_2).* ***i****,****j****, Average energy expenditure during light hours (day).* ***k****,****l****, Average energy expenditure during dark hours (night). For* ***c****-****l****, all measurements were performed on each day of the FMD cycle until refeeding on day 10. All data are shown as mean ± s.e.m., n = 4 mice per group. Two-way ANOVA coupled with Bonferroni's multiple-comparisons tests was performed. P values associated with each pairwise comparisons can be found in Supplementary Table 2.*

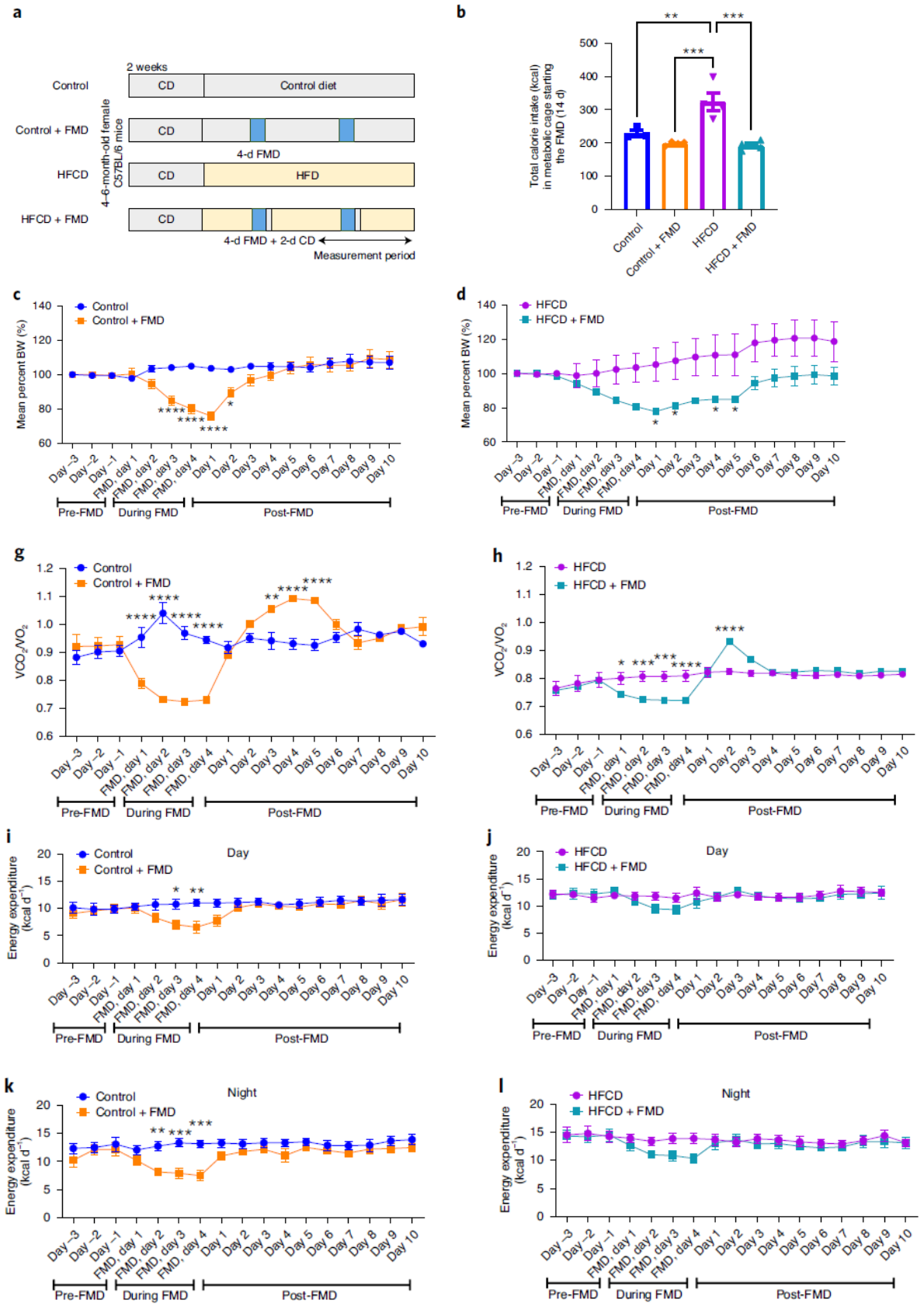

FMD cycles improve risk factors of metabolic syndrome and CVD. The reduction in adiposity in

HFCD + FMD-fed mice was not accompanied by lean body mass loss (Fig. 2a, one-way ANOVA, *P* value < 0.0001). Mice fed an HFCD had increases in body weight primarily due to increased body fat accumulation without any significant increase in lean mass. HFCD-fed mice also had a higher body fluid level, congruent with being heavier, than those in control and HFCD + FMD groups (Fig. 2a, one-way ANOVA, *P* value < 0.0001).

Although the serum cholesterol level increased slowly with age in all groups of mice, it increased faster in the HFCD group (Fig. 2b). Mice in HFCD and HFCD + FMD groups showed a similar level of serum cholesterol at 14 months (after four FMD cycles). However, HFCD + FMD-fed mice had cholesterol levels similar to those in the control diet group at 18 (after eight FMD cycles) and 33 months of age (after 23 FMD cycles), whereas cholesterol levels were almost four times higher in the HFCD group than those in the control group at 33 months (Fig. 2b, one-way ANOVA, *P* value < 0.0001). Serum triglyceride levels were not different between the groups after either ~8 months (eight cycles) or ~14 months (14 cycles) on diet (Fig. 2c), in line with previous reports in which an HFD had no effects on serum triglyceride levels in mice[16].

Serum ketone body levels were elevated only in the HFCD + FMD group 4 d after the end of the FMD, a signature of sustained fat catabolism resulting from periodic fasting (Fig. 2d, one-way ANOVA, *P* value = 0.0108). Mice on the control diet and the HFCD showed no difference in serum ketone body levels compared to baseline (Fig. 2d).

Leptin and ghrelin play an important role in the control of food intake and satiety; higher leptin levels promote hunger, and higher ghrelin levels promote satiety[17]. Mice on the HFCD had a higher level of serum leptin than those in both control and HFCD + FMD groups (Fig. 2e, one-way ANOVA, *P* value < 0.0001), while displaying the same level of ghrelin as control mice. By contrast, mice in the HFCD + FMD group showed a trend toward higher serum ghrelin levels (Fig. 2f, one-way ANOVA, *P* value = 0.0551).

High alanine transaminase activity is a marker for liver disease and is also associated with an increased incidence of CVD[18]. HFCD-fed mice showed a trend for elevated alanine transaminase activity, while those on the HFCD + FMD regimen had levels similar to those in mice on the control diet (Supplementary Fig. 1c, one-way ANOVA, *P* value = 0.1625). HFCD and HFCD + FMD groups showed higher liver weight than controls, but the HFCD group had a lower liver-to-body weight ratio than either control or HFCD + FMD groups, while the HFCD + FMD group had a liver-to-body weight ratio similar to that of the control group (Extended Data Fig. 2a, b). Histopathological analysis of the liver based on nonalcoholic steatohepatitis clinical research network guidelines[19] showed a high score (>3) for all groups (Extended Data Fig. 2c). The high histological score is possibly due to the advanced age of mice[20]. The HFCD + FMD group, however, displayed a trend toward decreased steatosis (Extended Data Fig. 2d).

In a separate group of C57BL6/JNia mice on a control diet, the HFCD or the HFCD + FMD (5-d FMD with a 2-d control diet) regimen, blood glucose, glucose tolerance (glucose tolerance test (GTT)) and insulin tolerance (insulin tolerance test (ITT)) were assessed. Mice on the HFCD showed a significantly elevated level of blood glucose after ~5 months, while mice undergoing cycles of the FMD (five cycles) with the HFCD had a blood glucose level slightly lower than even that of the control group (Fig. 2c, two-way ANOVA, *P* value < 0.0001). HFCD + FMD-fed mice also performed better in both the GTT and the ITT than the HFCD group and performed similarly to the control

group (Fig. 2h-k). The area under the curve (AUC) of glucose levels was elevated in the HFCD group in both the GTT and the ITT, but it was significantly lower in the HFCD + FMD group, similar to that of the control group (Fig. 2i,k, GTT, one-way ANOVA, *P* value = 0.0190; ITT, one-way ANOVA, *P* value = 0.0011).

Taken together, these results indicate that monthly 5-d FMD cycles prevent hypercholesterolaemia, hyperglycaemia and hyperleptinaemia caused by the obesogenic diet and also promote fat breakdown for at least 4 d following the end of the FMD cycle. Furthermore, cycles of the FMD improve the HFCD-induced impaired performance in GTTs and ITTs.

The FMD and metabolic regulation. To study the effect of the different dietary regimens on metabolism, individual mice were studied using metabolic cages. Four groups of mice were studied: mice on a control diet with or without FMD cycles and mice on an HFCD with or without FMD cycles. Mice underwent two cycles of the FMD (4-d FMD followed by 2 d of the control diet before switching to 24 d of the control or HFCD diet) (Fig. 3a). Measurements were recorded inside metabolic cages starting 3 d before the start of the second FMD cycle and continued until 10 d after the end of the FMD cycle. Total body weight, daily caloric intake, respiratory exchange ratio (RER) and caloric expenditure were measured.

Figure 4 - FMD cycles improve histological and physiological markers of cardiac health in HFCD-fed mice. ***a****, Representative immunofluorescence staining for isolectin B4 in myocardial cross-sections of 21-month-old mice. Mice were fed either a control diet, the HFCD or HFCD with periodic FMD (11 cycles). Tissues were collected 4 d after the end of the FMD cycle.* ***b****, Software-assisted quantification of the fluorescence intensity depicted in* ***a****. IB4, isolectin B4. n = 6 per group. One-way ANOVA, *P = 0.0104. Tukey's multiple-comparisons tests, control versus HFCD, P = 0.9407; control versus HFCD + FMD, P = 0.0284; HFCD versus HFCD + FMD, P = 0.0147.* ***c****, Representative Elastica van Gieson staining of elastic fibres.* ***d****, Software-assisted quantification of the aortic elastic lamina thickness depicted in* ***c****. One-way ANOVA, *P = 0.0166. Tukey's multiple-comparisons tests, control versus HFCD, *P = 0.0152; control versus HFCD + FMD, P = 0.568 (NS); HFCD versus HFCD + FMD, P = 0.0775. Control (n = 5), HFCD (n = 5), HFCD + FMD (n = 6).* ***e****, Representative H&E staining of aortas of mice fed the control diet, the HFCD or HFCD + FMD.* ***f****, Aortic wall thickness in μm measured from the H&E images depicted in* ***e****. One-way ANOVA, P value = 0.1915 (NS). Tukey's multiple-comparisons tests, control versus HFCD, P = 0.6823 (NS); control versus HFCD + FMD, P = 0.5617 (NS); HFCD versus HFCD + FMD, P = 0.1694 (NS). Control (n = 5), HFCD (n = 5), HFCD + FMD (n = 6).* ***g****, Representative H&E images of cardiomyocytes of mice fed the control diet, the HFCD or HFCD + FMD.* ***h****, The cross-sectional area of cardiomyocytes was quantified from H&E-stained sections (****g****) in control, HFCD-fed and HFCD + FMD-fed mice. One-way ANOVA, P value = 0.0663 (NS). Unpaired t-test, control versus HFCD, P = 0.4977 (NS); control versus HFCD + FMD, P = 0.0581 (NS); HFCD versus HFCD + FMD, *P = 0.0214. Control (n = 18), HFCD (n = 16), HFCD + FMD (n = 7).* ***i****, Representative echocardiographic images during peak stress and recovery after injecting dobutamine. Stress echocardiography was performed after 19 cycles of the FMD.* ***j****, Time to recovery from stress echocardiography measured in min (time taken to return to a heart rate at 120% of baseline). One-way ANOVA, *P = 0.0204. Tukey's multiple-comparisons tests, control versus HFCD, *P = 0.0176; control versus HFCD + FMD, P = 0.8752 (NS); HFCD versus HFCD + FMD, *P = 0.0317. Control (n = 10), HFCD (n = 3), HFCD + FMD (n = 12).* ***k****, EDV in different groups. One-way ANOVA, P = 0.3808 (NS). Control (n = 9), HFCD (n = 3), HFCD + FMD (n = 12).* ***l****, LVID-d in different groups. One-way ANOVA, P = 0.0520. Tukey's multiple-comparisons tests, control versus HFCD, P = 0.1262 (NS); control versus HFCD + FMD, P = 0.7462 (NS); HFCD versus HFCD + FMD, *P = 0.0413. Control (n = 9), HFCD (n = 3), HFCD + FMD (n = 12).* ***m****, Diastolic interventricular septal thickness (septum-d) in different groups. One-way ANOVA, P = 0.4740. Control (n = 9), HFCD (n = 3), HFCD + FMD (n = 12).* ***n****, LVPW-d in different groups. One-way ANOVA, P = 0.4404. Control (n = 9), HFCD (n = 3), HFCD + FMD*

(n = 12). ***o****, LV mass in different groups. One-way ANOVA, P = 0.1767 (NS). Control (n = 9), HFCD (n = 3), HFCD + FMD (n = 12). All data are shown as mean ± s.e.m.*

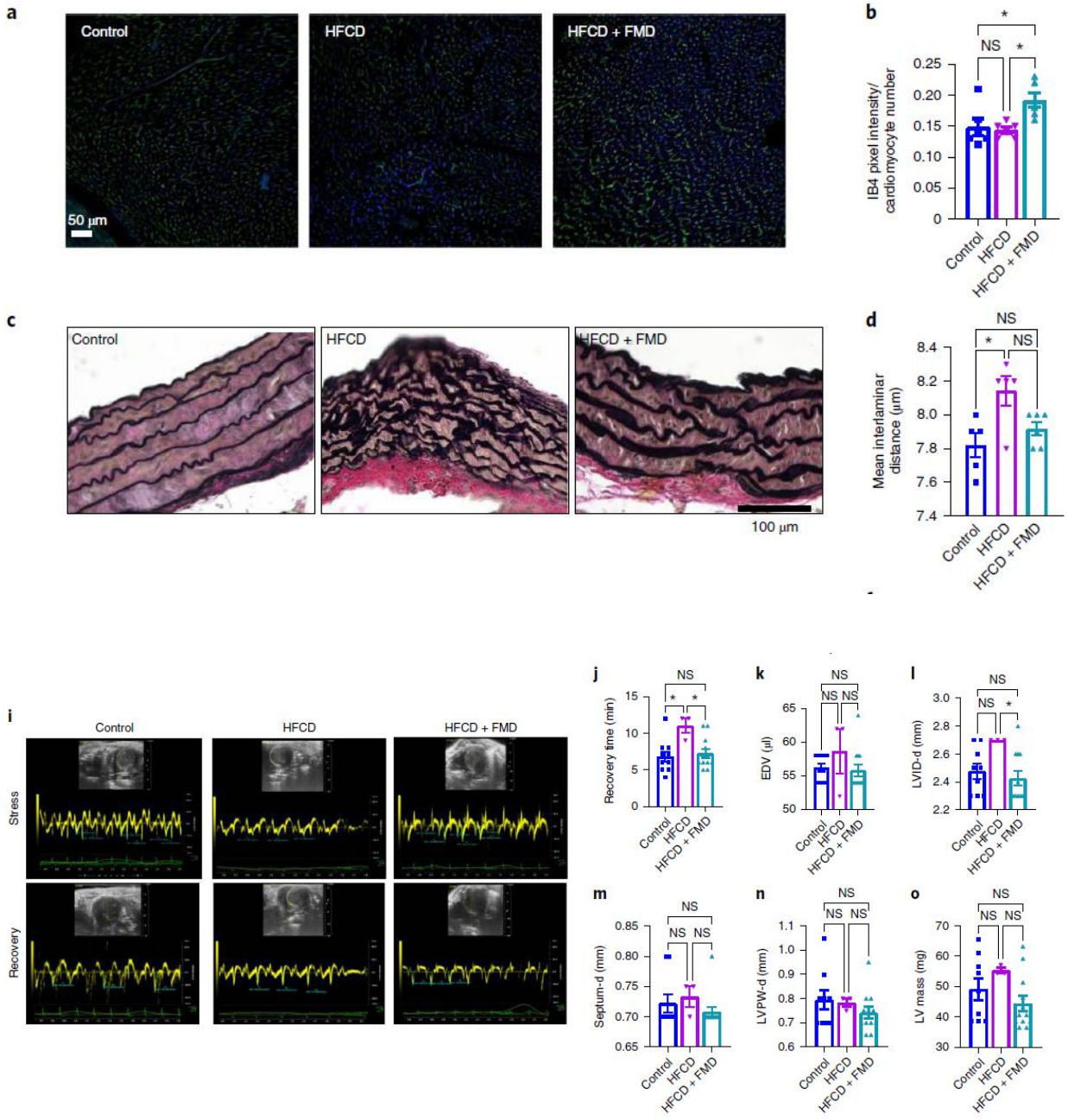

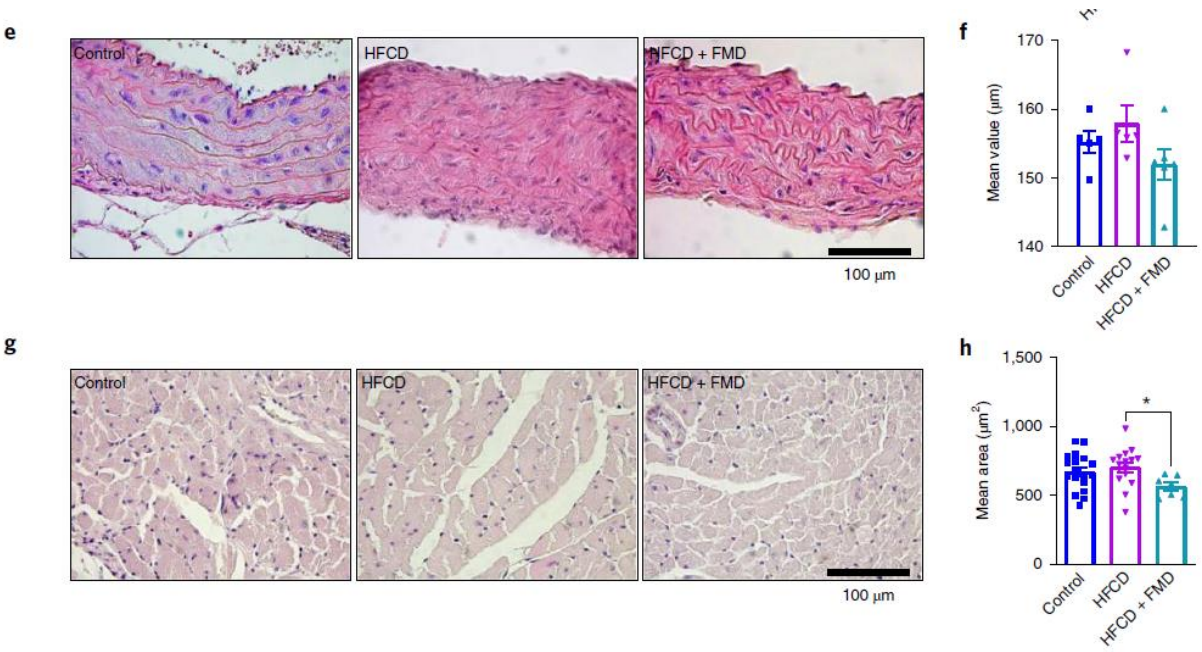

Mice in both control with FMD and HFCD + FMD groups lost body weight during the 4-d FMD; but, while mice in the control with FMD group regained the lost weight within 5 d of switching back to the control diet, mice in the HFCD + FMD group maintained reduced weight even after 10 d of refeeding with the HFCD diet (Fig. 3c,d). To further investigate weight regain in the control + FMD group and maintenance of lost weight in the HFCD + FMD group, we examined the calorie-intake data. Mice on the control + FMD diet started overeating after returning to the control diet at the end of the FMD cycle, resulting in higher caloric intake than that in control mice, while HFCD + FMD-fed mice ate the same amount of calories after the FMD as mice continuously on the HFCD, even though they had ad libitum access to food (Fig. 3e,f). This calorie intake in the HFCD + FMD group was maintained long after the end of the FMD cycle (Fig. 3f), suggesting a reprogramming of feeding habits by the FMD cycle, possibly associated with the reprogramming of fat catabolism indicated by sustained ketogenesis in the HFCD + FMD group but not in the HFCD group. To determine the net effect of this differential calorie intake between control + FMD-fed and HFCD + FMD-fed mice, total energy intake was determined in all groups. Food consumption was similar in control and control + FMD-fed mice, in agreement with the observation that, during the FMD period, fewer calories were consumed, but that, during the days following the FMD cycle, control + FMD-fed mice binged until reaching their normal body weight (Fig. 3b,c,e). In contrast, HFCD-fed mice consumed significantly higher amounts of calories than the other three groups (Fig. 3b, one-way ANOVA, *P* value = 0.0111). Mice on the HFCD + FMD ate significantly fewer calories than HFCD-fed mice, reaching a level similar to that of control and control + FMD-fed mice. These results indicate a 'limited food consumption' behaviour, in addition to a sustained ketogenic effect in HFCD + FMD-fed mice (Fig. 3b).

The RER is a measure of muscles' oxidative capacity as well as an indicator of primary substrate utilization for energy production; a high RER indicates predominant utilization of carbohydrates (RER = 1.0), and a low RER is indicative of predominant utilization of fat (RER = 0.7) as an energy source[21]. The range between 0.7 and 1.0 indicates a mixed use of substrates. During the FMD cycle, a greater use of fat as an energy source was observed in both control + FMD and HFCD + FMD groups, while mice on both control and HFCD diets showed a mixed-use pattern (Fig. 3g,h). This

shift in metabolism was reversed during the days following the FMD in control with FMD-fed mice, consistent with their higher calorie intake (Fig. 3e,g). In HFCD + FMD-fed mice, the switch from fat to carbohydrate utilization was not as clear on the days following the FMD, with only a slight increase in the RER on days 2 and 3 and a return to a mixed-use pattern similar to that observed with control and HFCD regimens (Fig. 3h).

Mice in all groups showed higher energy expenditure during the night than during the day, consistent with their nocturnal lifestyle (Fig. 3i-l). Mice in control + FMD and HFCD + FMD groups showed a similar energy expenditure during the day and at night compared to control and HFCD-fed mice, respectively, during the refeeding period and a lower expenditure during the fasting period (Fig. 3i-l). Thus, FMD cycles reprogramme the feeding behaviour of mice on the HFCD, which, together with an increase in fat breakdown, could justify the effects on adiposity and early mortality.

Periodic cycles of the FMD improve cardiac health in mice fed an HFCD. Capillary density is critical for proper blood supply to the heart muscles, and poor angiogenesis is associated with hypertrophy and heart failure[22]. Capillary density is also dependent on age and health status, with individuals who are older or who suffer from heart disease having lower capillary density than younger and healthy individuals[23]. Isolectin B4 staining to quantify capillary density showed greater capillary density in HFCD + FMD-fed mice than that in mice on either the control diet or the HFCD, consistent with angiogenesis and better cardiac health in the HFCD + FMD group (Fig. 4a,b, one-way ANOVA, *P* value = 0.0104).

Reduced arterial elasticity is a major risk factor for CVD and is a marker for cardiac ageing[24]. Quantification of elastic lamina thickness of the aorta by Elastica van Gieson staining revealed an increase in interlaminar distance in HFCD-fed mice, while mice on the HFCD + FMD regimen displayed interlaminar distance similar to that of the control group (Fig. 4c,d, one-way ANOVA, *P* value = 0.0166). Histological quantification of haematoxylin and eosin (H&E)-stained aortic sections revealed only a trend for increased thickness in HFCD-fed mice, while aortic wall thickness trended lower in HFCD + FMD-fed mice than in the other two groups (Fig. 4e,f). Collagen deposition affects arterial elasticity, which increases with age and is thought to contribute to progressive heart dysfunction[25]. While no difference was observed in aortic collagen I expression between the three groups (Extended Data Fig. 3a, b), levels of collagen III in the tissue were higher in the HFCD group than in the control group (Extended Data Fig. 3c, d, one-way ANOVA, *P* value = 0.0285), but the HFCD + FMD group showed collagen III levels similar to those in the control group.

Figure 5 - Restoration of mitochondrial energy metabolism gene expression by the FMD. a,b, *Venn diagrams showing genes differentially expressed between the different feeding groups in the heart (**a**) and VAT (**b**). The empirical Bayes moderated t-test was implemented in the limma package and corrected for multiple-hypothesis testing. DEGs were selected for each comparison based on cutoffs of absolute log2 (FC) > 1 (FC > 2) and adjusted P value (false discovery rate) < 0.05. **c**, Heatmap of RNA-seq expression z scores computed for genes that were differentially expressed (adjusted P value < 0.05 and absolute log2 (FC) > 1; FC > 2) only in the BD pairwise comparison in heart tissue. z scores were computed after clustering for each gene by subtracting the mean and then dividing by the s.d. C1–C5, control; H1–H5, HFCD; HF1–HF4, HFCD + FMD. **d**, Heatmap of RNA-seq expression z scores computed for DEGs found only in the BD pairwise comparison in VAT and involved in significantly enriched pathways as identified by gene ontology analysis. Adjusted P value < 0.05 and absolute*

log2 (FC) > 1.0 (FC > 2). ***e****, Gene ontology analysis of DEGs present only in the BD pairwise comparison in VAT. Adjusted (adj) P value < 0.05. El., eletron; mitoch., mitochondrial; BP, biological process; CC, cellular component; MF, molecular function.*

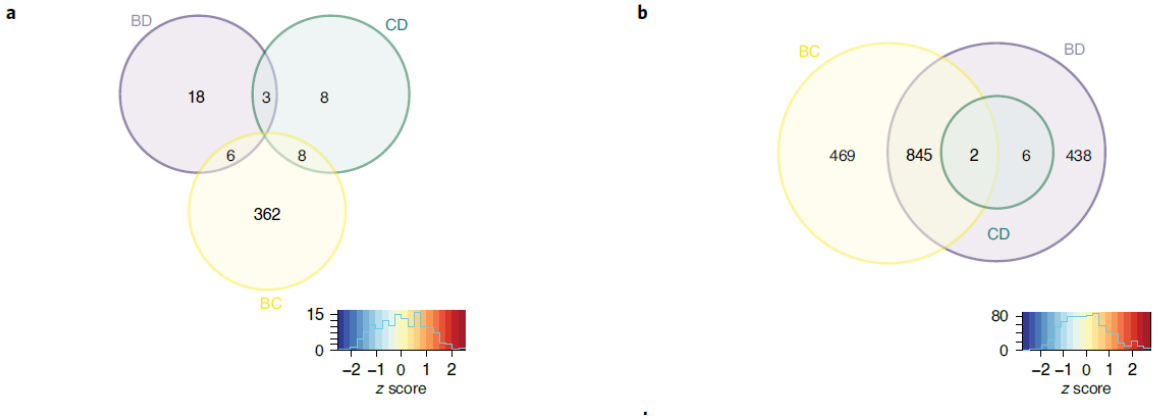

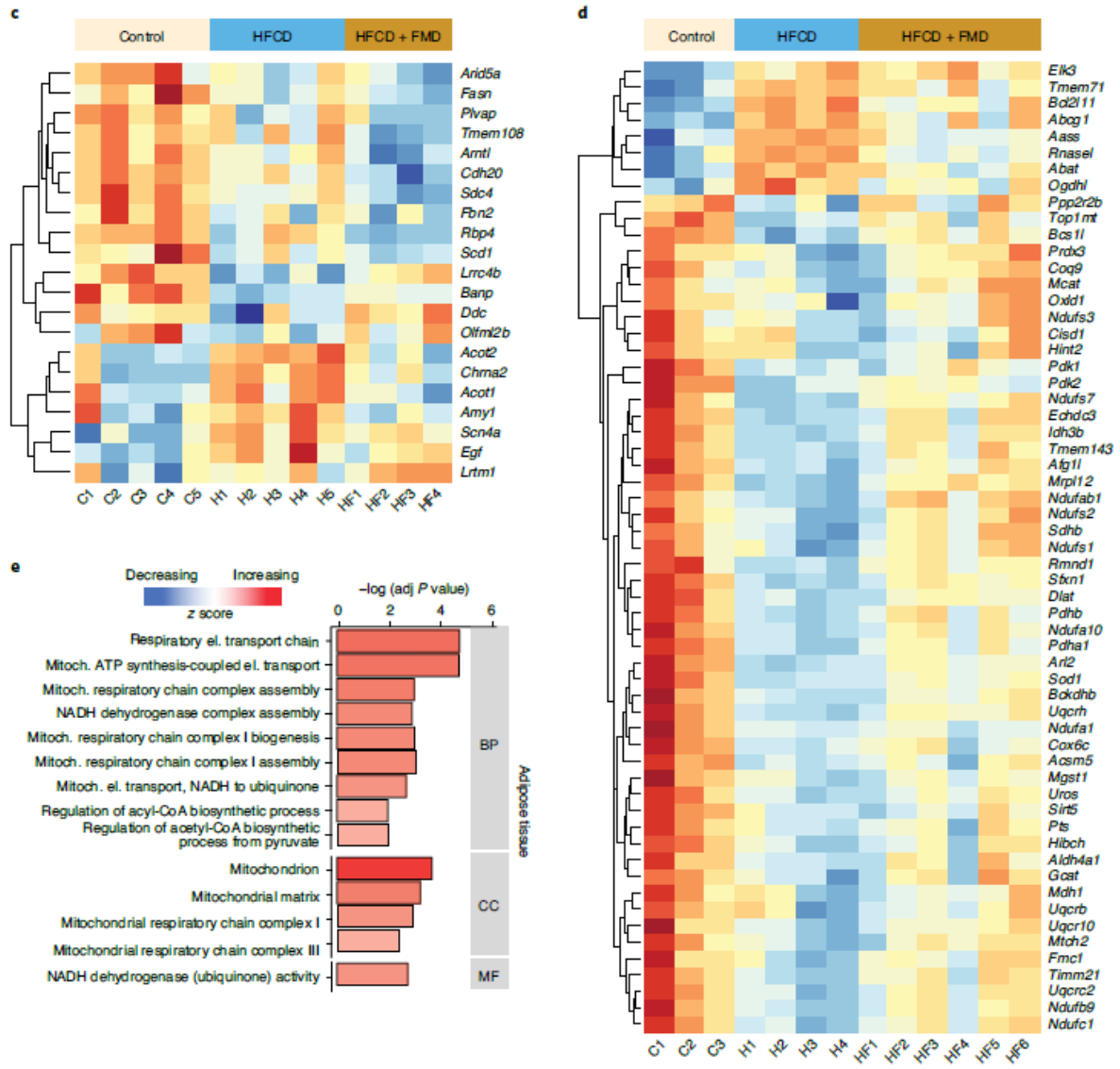

Figure 6 - FMD-mediated restoration of physiological and metabolic parameters in HFCD-fed mice. *HFCD-fed mice show decreased lifespan, cardiac stress tolerance, adipocyte mitochondrial biogenesis and metabolism, and increased body weight, adiposity, blood glucose levels, insulin resistance, leptin resistance, serum cholesterol levels, calorie intake and elastic lamina thickness, which is restored by cycles of the FMD in HFCD + FMD-fed mice. Additionally, FMD cycles lead to increases in serum ketone body levels and heart capillary density as well as decreases in aortic wall thickness in HFCD + FMD-fed mice compared to both control and HFCD-fed mice. The figure was made using BioRender*.

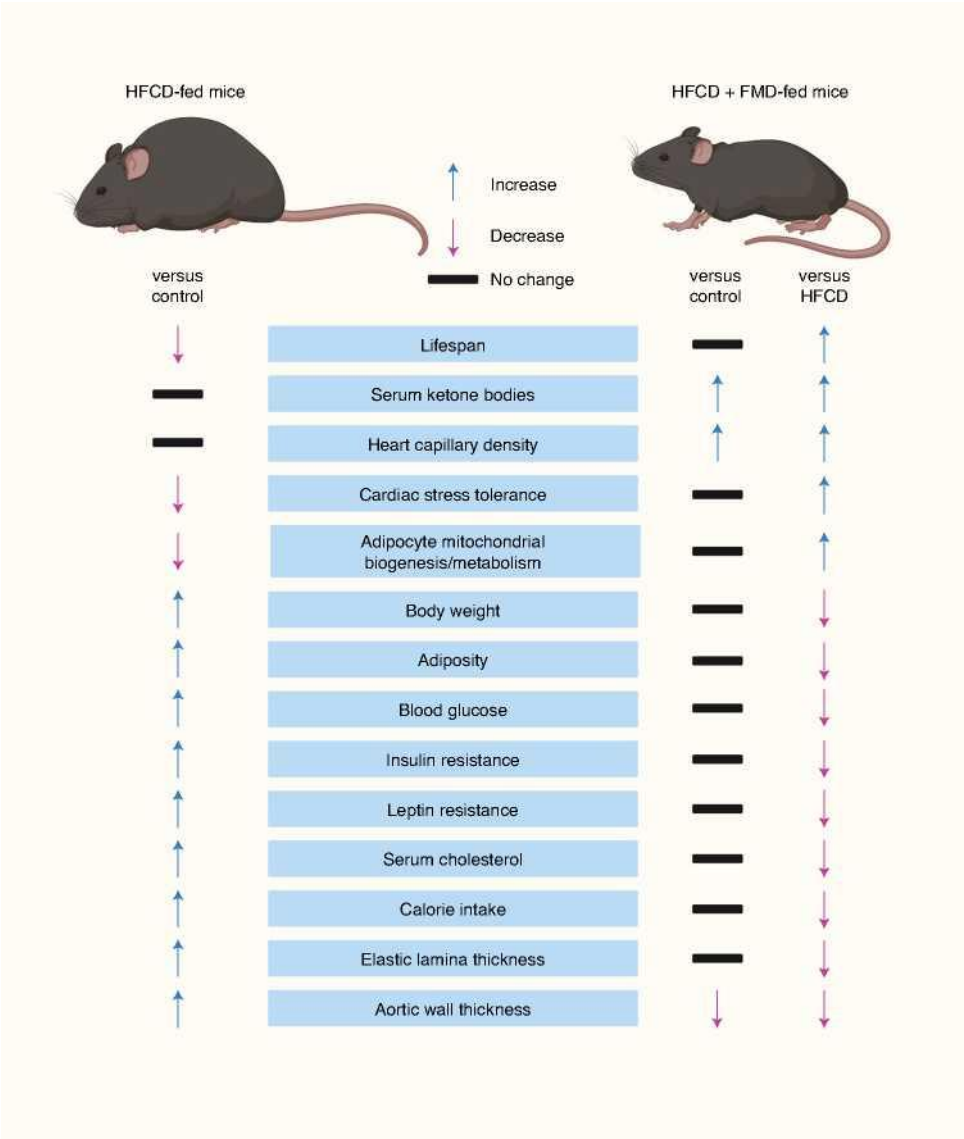

Myocardial hypertrophy has been associated with hypertension and heart failure in humans[26] and has been shown to precede heart failure in various animal models[27]. Quantification of the cross-sectional area of cardiomyocytes from H&E images of cardiac tissue showed an increase in cardiomyocyte size in HFCD-fed mice but a reduced size in HFCD + FMD-fed mice compared to the other two groups (Fig. 4g,h, one-way ANOVA, *P* value = 0.0663).

Stress echocardiography is performed to assess cardiac function after exposure to stress to reveal any subclinical disease that might not be evident under normal conditions[28]. Dobutamine acts as a cardiac stressor by stimulating βi adrenoceptors of the heart, resulting in increased contractility and cardiac output[29]. There was no discernable difference in cardiac chamber size or function at rest or peak stress. It is known that abnormalities in recovery from stress in dobutamine stress echocardiography may manifest as early indicators of cardiac dysfunction even when function appears normal at peak stress[30]. Heart rates of HFCD-fed mice but not mice on the HFCD + FMD regimen required a longer time to return to basal rates following peak stress compared to the control group (Fig. 4i,j, one-way ANOVA, *P* value = 0.0204). While no differences in end diastolic volume (EDV), diastolic left ventricle (LV) internal diameter (LVID-d), diastolic septum thickness,

diastolic LV posterior wall thickness (LVPW-d) or LV mass were observed at the end of the 12th cycle between the groups (Extended Data Fig. 4), after 19 cycles of the FMD, the HFCD + FMD group had a smaller LVID-d than that in the HFCD group, but comparable to that of the control group (Fig. 4l, one-way ANOVA, *P* value = 0.052; Tukey's multiple-comparisons test, HFCD versus HFCD + FMD, *P* = 0.0413). There was also a trend for increased EDV, septum thickness and LV mass in the HFCD group after 19 cycles than those in controls, whereas the HFCD + FMD group displayed levels comparable to those of the control group or lower (Fig. 4k,m,o). Also, we observed a trend for reduction in the LVPW after 19 cycles in the HFCD + FMD group compared to that of both control and HFCD groups (Fig. 4n). These observations indicate deterioration of heart function in the HFCD group, which is prevented by FMD cycles. Taken together, these results indicate that FMD cycles promote vascularization and prevent damage caused by the HFCD in the heart.

FMD cycles promote mitochondrial metabolism in mice fed an HFCD. To explore changes in the gene expression pattern and to highlight genes that may be involved in cardiac and metabolic health as well as longevity, we performed RNA sequencing (RNA-seq) on the heart and VAT from 21-month-old mice (4 d after the end of 11 cycles on their respective diets, *n = 3-6* per group). All genes that had an adjusted *P* value < 0.05 and absolute $\log_2$ (fold change (FC)) > 1.0 (FC > 2) were considered to be differentially expressed. We then performed a pairwise comparison between control versus HFCD (BD), HFCD versus HFCD + FMD (DC) and control versus HFCD + FMD (BC) to identify differentially expressed genes (DEGs) that were unique or shared between the groups.

In the heart tissue, 27, 376 and 19 genes were differentially expressed in BD, BC and DC comparisons, respectively (Fig. 5a). By contrast, 1,291, 1,316 and eight genes were found to be differentially expressed in the VAT of BD, BC and DC comparisons, respectively (Fig. 5b). To identify the gene expression change induced by the HFCD but not by the HFCD + FMD regimen, we examined genes differentially expressed in the BD comparison that were absent in the BC pairwise comparison. This analysis identified 21 genes in the heart and 444 genes in adipose tissue for which expression was differentially impacted as a result of the HFCD (Fig. 5c and Supplementary Fig. 1). A heatmap of these 21 genes in the heart, including *Lrrc4b*, *Banp*, *Ddc*, *Olfml2b*, *Acot1* and *Amy1*, is depicted in Fig. 5c. Among these significantly DEGs, Kyoto Encyclopedia of Genes and Genomes (KEGG) and WikiPathways analyses identified biosynthesis of unsaturated fatty acids and cholesterol metabolism (*Acot1* and *Acot2*) pathways as upregulated and the fatty acid biosynthesis (*Fasn* and *Scd1*) pathway as downregulated in the heart of HFCD-fed mice (adjusted *P* value < 0.05) (Extended Data Figs. 5a and 6a).

Next, we analysed the heatmap of the 444 genes differentially expressed in the adipose tissue of HFCD-fed versus control mice (Supplementary Fig. 1). Interestingly, the expression level of most of these genes had a similar signature in HFCD + FMD (4 d following the end of the FMD) and control groups (Supplementary Fig. 1). Gene ontology analysis showed an enrichment of genes involved in mitochondrial metabolism, acetyl-CoA biosynthesis and NADH dehydrogenase activity with downregulated expression in HFCD-fed mice but with expression restored or partially restored by the HFCD + FMD regimen (adjusted *P* value < 0.05) (Fig. 5d,e). KEGG and WikiPathways analyses identified a number of differentially regulated pathways including those involved in oxidative phosphorylation, the tricarboxylic acid cycle, retrograde endocannabinoid signalling, thermogenesis, nonalcoholic fatty liver disease, Parkinson's disease and Alzheimer's disease (adjusted *P* value < 0.05) (Extended Data Fig. 5b). Expression levels of the genes enriched in these

pathways are depicted in Extended Data Fig. 6b, c. These results are consistent with fat cell reprogramming and a high level of oxidative phosphorylation after a series of FMD cycles.

Discussion

In the current study, we observed that the HFCD diet led to increased obesity, blood glucose levels, cholesterol levels, leptin levels and poor glucose and insulin tolerance as well as cardiac damage resulting in decreased survival as compared to those in mice fed a control diet, in agreement with previous studies[31-34]. While many nutritional interventions have been studied for their efficacy against obesity and CVD in both mice and humans, studies on the effects or benefits of short and periodic cycles of fasting or FMDs on obesity and obesogenic diets are lacking[35-38]. Rusli et al. studied the effect of alternate week intermittent calorie restriction in HFD-fed mice and observed partial reversal of the effects of the HFD[38]. The limitation of most effective diets, such as the Mediterranean or ketogenic diet, is that they require often radical and daily changes in dietary habits, which results in very low long-term compliance. Notably, Newman et al.[37] showed that both the HFD and the ketogenic diet can be obesogenic and correlate with decreased survival when given continuously, while alternate week feeding of the HFD or the ketogenic diet with a control diet reduces weight gain and prevents early mortality. However, even the long-term use of an alternate week diet is likely to result in low long-term compliance, underscoring the need for nutritional interventions to affect obesity and ageing while limiting the compliance burden, thus allowing long-term use. In the current study, 5 d of the FMD per month followed by 2 d on a regular diet were effective in preventing obesity and the negative effects of a lifelong HFCD on CVD risk and lifespan.

Serum cholesterol levels have long been associated with CVD and increased mortality[39]. While the HFCD + FMD group had serum cholesterol levels similar to those of the HFCD group at 14 months of age, these levels progressively increased in the HFCD group but not in the HFCD + FMD group as mice aged. The increase in cholesterol levels in the HFCD model occurred slowly and progressively, requiring more than 8 months to become significantly higher than those in the control but never reaching significance in the HFCD + FMD group. Similar effects were observed for weight and obesity. Interestingly, mice on the HFCD + FMD diet showed elevated levels of ketone bodies even 4 d after the end of the FMD cycle. Because high ketone body levels have been implicated in counteracting age-related cardiac remodelling, these results may explain part of the beneficial effects of FMD cycles[40]. Elevated levels of ketone bodies are also observed during calorie restriction and have been proposed to mimic the pro-longevity effects of calorie restriction itself[41]. The observations that circulating ketone body levels remain elevated and that the activity of many oxidative phosphorylation processes was increased in adipocytes 4 d after the end of the FMD indicate a sustained fat catabolism that, together with the reduced feeding behaviour, can explain the reduced weight in the HFCD + FMD group. However, an RER typical of fat-based metabolism was not observed after the FMD, indicating that skeletal muscle is unlikely to be the main site of fat metabolism, and raising the possibility that increased ketone bodies after the FMD cycles are being used primarily by the nervous system or other organs.

Mechanisms contributing to weight regain following behavioural interventions achieved by different diets include adipose cellularity, leptin and ghrelin levels, energy metabolism and neural responsivity[42]. Several studies have shown that dietary restriction-induced weight loss and regain

(weight cycling) can cause weight loss but has been associated with poor glucose tolerance[42-44]. Here we show that cycles of the FMD improve glucose and insulin tolerance in mice fed an HFCD. Mice in the HFCD + FMD group showed minimal changes in energy expenditure during the FMD cycle possibly due to greater fat reserves, which would compensate for the reduced calorie intake during the FMD (Fig. 3i-l). Mice fed a control diet and subjected to FMD cycles showed a compensatory eating behaviour after the FMD that resulted in weight regain to pre-FMD levels, whereas no such compensatory eating behaviour was observed in HFCD-fed mice following the FMD cycle (Fig. 3c-f). This suggests an alteration of eating behaviour leading to lower overall calorie intake in HFCD + FMD-fed mice that contributed to long-term maintenance of relatively low body weight even after feeding ad libitum on an HFCD for most of their lifetime (Fig. 1e,g). This could be in part controlled by reduced leptin levels and increased ghrelin levels induced by the FMD. This reprogramming of eating behaviour was not observed in human trials of frequent and intermittent fasting or continuous calorie restriction[45,46] but was anecdotally observed in our periodic FMD trial[9]. It will be interesting to formally test whether periodic FMD cycles can alter post-fasting eating behaviour in humans. Changing long-term dietary habits requires lifestyle changes that have been shown to be too difficult to follow by several studies dealing with long-term weight loss maintenance in obese individuals42. Thus, we believe that FMD cycles carried out two to four times a year would be much easier than permanent and major dietary changes, although more frequent use may lead to lower compliance[9].

We show higher capillary density in HFCD + FMD-fed mice than that in mice fed the HFCD or the control diet, an effect that was also seen in other rodent studies of long-term calorie restriction[47,48]. Long-term calorie restriction inhibits cardiomyocyte hypertrophy and aortic wall thickening and promotes better performance during dobutamine stress echocardiography[49]. In our study, the 5 d per month FMD regimen could also decrease cardiomyocyte size and aortic wall thickness as well as promote a faster recovery time in the stress echocardiography test in HFCD-fed mice.

Gene ontology analysis of DEGs in the heart did not show any significantly altered pathways in response to FMD cycles in HFCD- fed mice, while KEGG and WikiPathways identified enrichment of genes implicated in unsaturated fatty acid biosynthesis and cholesterol metabolism pathways in HFCD versus HFCD + FMD groups. A previous study on continuous calorie restriction also reported significant expression changes in only one gene, underscoring limited long-term effects of dietary restrictions on the heart transcriptome[50].

By contrast, gene ontology in the VAT identified an enrichment of many pathways involved in mitochondrial metabolism and biogenesis in response to the FMD in HFCD-fed mice, underscoring a strong association between mitochondrial activity and biogenesis in adipocytes and reduction of fat mass. Increased mitochondrial mass and biogenesis in adipose tissue was previously reported upon long-term continuous calorie restriction[50-52]. Remarkably, our study shows that the FMD induces long-term changes in the adipose transcriptome lasting for days after the end of FMD restriction and while feeding ad libitum, in agreement with sustained fat catabolism and ketogenesis. Obesity is considered a driver of mitochondrial dysfunction in adipocytes, leading to metabolic complications and type 2 diabetes[53]. Fat-specific insulin receptor knock-out (FIRKO) mice that mimic the effects of long-term calorie restriction, such as increased lifespan and lean body mass, also show elevated expression of genes involved in glycolysis, the tricarboxylic acid cycle, β-oxidation and oxidative phosphorylation in white adipose tissue as compared to that in

control mice[54].

In summary, FMD cycles induced major gene expression changes in adipocytes leading to long-term activation of adipocyte metabolism, fat catabolism, ketone body generation and weight loss. These changes were associated with improvement in heart function and protection as well as reduced levels of cholesterol (Fig. 6). The role of three monthly FMD cycles in reducing visceral adiposity and cholesterol levels in humanss[9], together with our results in mice, raise the possibility that long-term activation of fat catabolism during the periods following FMD cycles may also occur in humans and contribute to the reduction in CVD-risk factors.

In summary, our study shows that a monthly cycle of the FMD lasting 5 d and followed by 2 d of a normal diet in a mouse model of DIO not only reverses or prevents obesity but also restores a normal lifespan. This effect of the FMD appears to be mediated, in part, by spontaneous reprogramming of eating behaviour in the HFCD + FMD group, resulting in a lack of compensatory eating and weight regain usually observed in other calorie-restriction-driven weight loss programmes. Notably, unlike the effect of the great majority of calorie-restriction interventions, the reversal of HFCD-dependent obesity by FMD cycles was not accompanied by a reduction in lean body mass. The ability of short FMD cycles to increase mitochondrial metabolism and biogenesis in adipose tissue and augment serum ketone body levels raises the possibility that, in addition to the altered spontaneous feeding behaviour, a metabolic reprogramming toward fat catabolism contributes to weight loss. However, the lack of prolonged fat-based metabolism in the period after the FMD indicates that additional studies are necessary to shed light on the mechanisms responsible for the positive effects of the FMD counteracting the HFCD.

Methods

Experimental model. *Animals and husbandry.* All animal protocols were approved by the Institutional Animal Care and Use Committee of the University of Southern California (USC). Female C57BL/6J and C57BL/6JNia mice (9-11 months old) were procured from Jackson Laboratory and the National Institute on Aging, respectively. Mice were maintained in a pathogen-free environment and housed in clear shoebox cages in groups with constant temperature (71-73 °F) and humidity (30-60%), a 12-h-12-h light-dark cycle and access to water at all times. Mice were fed a control diet (D12450J, OpenSource Diets) for 2 weeks for acclimatization at the beginning of the study. Unless otherwise mentioned, mice were fed the same control diet ad libitum during the study. Mice were fasted for 3-4 h before blood collection for biochemical analysis.

Dietary intervention. Age-matched mice (9-11 months old) were distributed among three experimental groups in similar proportions at the beginning of the study. Following the 2-week observation period and acclimatization to a control diet, mice were maintained either on that diet (D12450J) or put on an HFCD (D12492, OpenSource Diets). A third group of mice was fed an HFCD diet with a monthly cycle of 5 d of the FMD (HFCD + FMD) for the first five cycles. Because the sudden change from the low-calorie FMD to the high-calorie HFCD was not well tolerated by mice in the HFCD + FMD group during the initial five cycles, we modified the refeeding period starting at cycle 6 as follows: at the completion of the 5-d FMD, mice were put on the control diet (D12450J) for 2 d before switching to the HFCD. Moreover, based on our previous observation of lower tolerance to the FMD in old age[10], the 5-d FMD period was reduced to 4 d during cycles 21-23

(Extended Data Fig. 1a). Mouse weight was recorded weekly except when on the FMD, during which it was recorded daily. Daily calorie intake was determined by monitoring the food intake of mice (average daily consumption per cage) before the start of the FMD. The FMD provides 50% of the daily calorie requirement on day 1 and 10% of the calorie requirement on days 2-5. The ingredients of the control diet, the HFCD and the FMD as well as their calorie densities are listed in Supplementary Table 1.

A timeline of assays or tests performed is shown in Extended Data Fig. 1b.

Body composition. Fat mass, lean mass and fluid levels were quantified using the Bruker Minispec Live Mice Analyzer LFII with standard settings.

Blood glucose. Blood glucose levels were measured after 4-6 h of fasting using the Precision Xtra Blood Glucose Meter kit and glucose test strips (Abbott) according to the manufacturer's protocol. Blood samples were obtained by puncturing the tail vein of mice.

Serum leptin, ghrelin, triglyceride and cholesterol quantification. Serum was obtained from mice after 3-4 h of fasting and used on the same day or stored at -80 °C. Serum leptin (Mouse Leptin ELISA kit, RAB0334, Sigma-Aldrich), ghrelin (Rat/Mouse Ghrelin (total) ELISA kit, EZRGRT, Sigma-Aldrich) and triglyceride (Triglyceride Colorimetric Assay kit, 10010303, Cayman Chemical) quantification was performed according to manufacturers' protocols.

Oral glucose tolerance test and intraperitoneal insulin tolerance test.

C57BL/6JNia mice were used for GTT and ITT experiments. Age-matched mice (9.5 months old) were distributed among three experimental groups (five mice per group) in similar proportions at the beginning of the study. Following the 2-week observation period and acclimatization to a control diet, mice were maintained either on that diet (D12450J) or put on an HFCD (D12492, OpenSource Diets). A third group of mice was fed an HFCD with a monthly cycle of 5 d of the FMD (HFCD + FMD) followed by 2 d of the control diet before switching back to the HFD based on observations from previous experiments.

Oral glucose tolerance test. The oral GTT was performed according to a published protocol[56]. Briefly, mice fasted for 6 h before the test. Body weight was measured, and fasting glucose levels were recorded. Mice were then administered 2 g glucose per kg of body weight by oral gavage, and blood glucose levels were measured at 15 min, 30 min, 60 min and 120 min.

Intraperitoneal insulin tolerance test. The intraperitoneal ITT was performed according to a published protocol[56]. Briefly, mice fasted for 6 h before the test. Body weight was measured, and fasting glucose levels were recorded. Mice were then administered 0.5 U insulin per kg (Humulin R U-100, Lilly) of body weight by intraperitoneal injection, and blood glucose levels were measured at 15 min, 30 min, 60 min and 120 min.

Serum cholesterol. Serum cholesterol levels were measured using the Cholesterol Fluorometric Assay kit (10007640, Cayman Chemical) according to the manufacturer's protocol.

Alanine transaminase activity. Alanine transaminase activity was measured using the EnzyChrom Alanine Transaminase Assay kit (BioAssay Systems) according to the manufacturer's protocol.

Ketone bodies. Ketone bodies were quantified using the β-Hydroxybutyrate (Ketone Body) Assay kit (700190, Cayman Chemical) according to the manufacturer's protocol.

In vivo magnetic resonance imaging. MRI scans were performed at the Molecular Imaging Center using the Aspect M7 scanner. Before acquisition, animals were administered gadolinium contrast agent intravenously via the tail vein under inhalant anaesthesia. Animals were placed into an imaging coil equipped to deliver an inhalant anaesthetic using the nose cone method and a vaporiser with scan times up to 30 min. After induction, mice were transferred to a fully shielded small animal 1-tesla MRI system (Aspect Imaging) for MRI scans, while being maintained on 1-2% isoflurane in oxygen via the nose. Animals were allowed to recover after imaging was complete, at which time they were returned to the vivarium using transfer cages. Fat volume was calculated using T1- and T2-weighted MRI images and Amira software for 3D visualization, processing and analysis (Thermo Fisher Scientific).

Stress echocardiography. The dobutamine stress echocardiography protocol was adapted from standard human protocols[30,57]. Briefly, anaesthetized mice were maintained under 1-2% isoflurane in medical oxygen on a temperature-controlled platform with ECG leads. Internal body core temperature was monitored using a rectal probe cleaned with alcohol pads. Physiological parameters (that is, the heart rate) were monitored by ECG. After placing the animal on the platform of the Ultrasound Vevo 2100 system (VisualSonics), ultrasound gel was applied to the chest area to visualize the heart. A tail vein catheter was inserted in advance for drug infusion using a Harvard infusion-withdrawal pump set to deliver dobutamine at 1.5 µg min^{-1} per kg. LV 2D and M-mode images were obtained at baseline, at peak stress and until the heart rate recovered to 120% of baseline. After completing imaging, echo data were analysed offline by an expert.

Metabolic parameters. Metabolic cages (TSE PhenoMaster System) were used to simultaneously measure energy expenditure, physical activity, indirect calorimetry and food and water intake in awake singly caged mice. The experiment non-invasively measures O_2 consumption and CO_2 production and calculates the RER to reflect energy expenditure in individual mice. Quantitative measurement of horizontal and vertical movement (*xyz* axis) as an index of physical activity over a given period of time was also recorded. Female C57BL/6J mice (4-6 months old) underwent two cycles of the FMD (4 d of the FMD, 2 d of the control diet and 24 d of the HFCD). Food access during the ad libitum phase was monitored automatically by weight sensors, while, during diet change and the FMD phase, we fed mice every day with the specified amount of food. Data recording had to be stopped very briefly to add food during the FMD and during diet switching but did interfere with overall data collection. Recording inside the metabolic cages began 3 d before the start of the second FMD cycle and continued until 10 d after completion of the FMD cycle for a total of 17 d. Experiments were carried out at the USC Leonard Davis School Aging Murine Phenotyping Core Facility.

Histology. The heart and aorta were collected and then fixed with 4% paraformaldehyde overnight. Serial sections of the myocardium were obtained at 6-µm intervals for paraffin-embedded tissue. Serial sections were stained with H&E (1051750 and 109844, respectively, Sigma-Aldrich) for analysis of cardiomyocyte cross-sectional areas. Serial 7-µm sections of aortic tissue were stained with the Accustain Elastin Verhoeff van Gieson kit (HT25A-1KT, Sigma-Aldrich) according to the manufacturer's protocol.

Immunofluorescence was performed as reported previously[58]. Paraffin sections were deparaffinized and rehydrated, and then antigen retrieval was performed using citrate buffer, pH 6,

at 70 °C for 10 min. After blocking with BSA (Sigma-Aldrich) for 30 min, slides were incubated with primary antibodies directed against isolectin B4 (Alexa Fluor 488 Conjugate, I21411, Thermo Fisher Scientific, 1:100 dilution), collagen I (mouse monoclonal (3G3) to collagen I, ab88147, Abcam, 1:50 dilution) and collagen III (rabbit polyclonal anti-collagen III, SAB4500367, Sigma-Aldrich, 1:50 dilution) overnight at 4 °C. The next day, samples were incubated with a species-specific fluorescent secondary antibody (anti-rabbit IgG-FITC antibody produced in goat, F0382, Sigma-Aldrich, 1:100 dilution; anti-mouse IgG-Atto 488 antibody produced in goat, 62197, Sigma-Aldrich, 1:150 dilution). Sections were stained with DAPI and were mounted using Mowiol (Mowiol 4-88, 81381, Sigma-Aldrich). Images were captured using the Leica TCS SP8 Confocal Microscope (Leica Microsystems). The isolectin B4 staining intensity of different cardiac microvessels was expressed as the mean pixel intensity normalized to the number of cardiomyocytes. This number was obtained from histological evaluation of the corresponding serial section (H&E). Staining intensities for collagen I and collagen III in the aortic wall (adventitia and media) were expressed as the mean pixel intensity normalized to the cross-sectional area using Leica Application Suite Advanced Fluorescence software[58]. Aortic wall thickness and cardiomyocyte cross-sectional areas were quantified using ImageJ software (NIH). Cardiomyocyte cross-sectional area was measured only along the short axis.

Histological scoring. Sections from mouse liver samples were stained with H&E and Masson trichrome for histological evaluation. In this histological analysis, we performed scoring using the histological scoring system for nonalcoholic fatty liver disease as a reference as previously described by Kleiner and Brunt[19]. For our study, we obtained a score by applying a semiquantitative evaluation of three histological features (steatosis, lobular inflammation and fibrosis). Steatosis was classified as grade 0 when present in <5% of the tissue, grade 1 when present in between 5% and 33% of the liver parenchyma, grade 2 when present in 33-66% of tissue and grade 3 when present in >66% of liver tissue. Lobular inflammation was evaluated based on the presence and number of inflammatory cell aggregates (foci) as follows: 0, no foci; 1, more than two foci per 200x field; 2, two to four foci per 200X field; 3, more than four foci per 200x field. Fibrosis was scored based on the presence of fibrous thickening as follows: 0, no fibrosis; 1, perisinusoidal fibrosis; 2, perisinusoidal, portal and periportal fibrosis; 3, bridging fibrosis; 4, cirrhosis.

RNA sequencing and analysis. *Library preparation and sequencing.* Samples were extracted using the RNeasy Mini kit following the manufacturer's instructions (Qiagen). Libraries were constructed using the KAPA RNA Hyper with RiboErase (HMR) kit (Roche) and sequenced on an Illumina HiSeq 3000 machine.

RNA-seq analyses. Sample alignment was performed using STAR 2.5.3 (ref. [59]) against the mouse genome (mm10). Differential expression analysis was performed using the limma package (R version 3.5.3)[60]. For each tissue (VAT and heart), we filtered out reads with low counts (counts per million (CPM) < 0.5) and explored the data to check for outliers and batch effects. The remaining genes and samples were normalized using trimmed mean of *M* values in the edgeR package[61] in R. In total, 15,145 and 13,238 genes remained after filtration for adipose and heart tissue, respectively. Reads were then processed by the voom method with quality weight in limma to convert them into $\log_2$ (CPM) with associated precision weights[60,62]. We then performed pairwise comparisons between control and HFCD, HFCD and HFCD + FMD, control and HFCD + FMD and

baseline and HFCD + FMD.

DEGs were selected for each comparison based on cutoffs of absolute $\log_2$ (FC) > 1 and adjusted *P* value < 0.05, after which Venn diagrams were produced using gene name lists and the VennDiagram R package[63].

Heatmaps of RNA-seq expression *z* scores of DEGs were generated using the heatmap.2 package (http://www.rdocumentation.org/packages/gplots/ versions/3.0.1.1/topics/heatmap.2) in R to present DEGs in the control versus HFCD comparison, showing only the ones not shared with the control versus HFCD + FMD comparison. *z* scores were computed after clustering for each gene by subtracting the mean and then dividing by the s.d.

To analyse DEGs at the functional level, gene ontology, KEGG and WikiPathways pathway enrichment analyses were performed using the Enrichr online tool[64, 65]. Significantly enriched (adjusted *P* value < 0.05) gene ontology terms (biological process, molecular function and cellular component) and pathways were identified. For gene ontology analysis, results were visualized using the R package GOplot[66].

Quantification and statistical analysis. No statistical methods were used to predetermine sample size. Experiments were not randomized, and investigators were not blinded to allocation during experiments and outcome assessments. Statistical analysis was performed using GraphPad Prism 8 (GraphPad Software). In all analyses, *P* < 0.05 was considered statistically significant, and the significance of *P* values was annotated as in GraphPad (≥ 0.05 (NS), 0.01-0.05 (*), 0.001-0.01 (**), 0.0001-0.001 (***), <0.0001 (****)).

Reporting Summary

Further information on research design is available in the Nature Research Reporting Summary linked to this article.

Data availability

RNA-seq data have been deposited in NCBI's Gene Expression Omnibus[55] under the accession code GSE163060. Source data are provided with this paper.

Received: 29 December 2020; Accepted: 2 September 2021;

Published online: 14 October 2021

References

1. *National Center for Health Statistics: National Health and Nutrition Examination Survey 2020* (CDC, 2020).
2. Fryar, C. D., Carroll, M. D. & Ogden, C. L. *Prevalence of overweight, obesity, and extreme obesity among adults aged 20 and over: United States, 1960-1962 through 2013-2014* (National Center for Health Statistics, CDC, 2016).
3. Schrauwen, P. & Westerterp, K. R. The role of high-fat diets and physical activity in the regulation of body weight. *Br. J. Nutr.* 84, 417-427 (2000).
4. Després, J.-P. & Lemieux, I. Abdominal obesity and metabolic syndrome. *Nature* 444, 881-887

(2006).

5. Astrup, A. The role of dietary fat in obesity. *Semin. Vasc. Med.* 5, 40-47 (2005).

6. Buettner, R., Scholmerich, J. & Bollheimer, L. C. High-fat diets: modeling the metabolic disorders of human obesity in rodents. *Obesity* 15, 798-808 (2007).

7. Hu, S. et al. Dietary fat, but not protein or carbohydrate, regulates energy intake and causes adiposity in mice. *Cell Metab.* 28, 415-431 (2018).

8. Longo, V. D. & Mattson, M. P. Fasting: molecular mechanisms and clinical applications. *Cell Metab.* 19, 181-192 (2014).

9. Wei, M. et al. Fasting-mimicking diet and markers/risk factors for aging, diabetes, cancer, and cardiovascular disease. *Sci. Transl. Med.* 9, eaai8700 (2017).

10. Brandhorst, S. et al. A periodic diet that mimics fasting promotes multi-system regeneration, enhanced cognitive performance, and healthspan. *Cell Metab.* 22, 86-99 (2015).

11. Choi, I. Y. et al. A diet mimicking fasting promotes regeneration and reduces autoimmunity and multiple sclerosis symptoms. *Cell Rep.* 15, 2136-2146 (2016).

12. Cheng, C.-W et al. Fasting-mimicking diet promotes Ngn3-driven P-cell regeneration to reverse diabetes. *Cell* 168, 775-788 (2017).

13. Di Biase, S. et al. Fasting-mimicking diet reduces HO-1 to promote T cell-mediated tumor cytotoxicity. *Cancer Cell* 30, 136-146 (2016).

14. Rangan, P. et al. Supplementary-fasting-mimicking diet modulates microbiota and promotes intestinal regeneration to reduce inflammatory bowel disease pathology. *Cell Rep.* 26, 2704-2719 (2019).

15. Ingvorsen, C., Karp, N. A. & Lelliott, C. J. The role of sex and body weight on the metabolic effects of high-fat diet in C57BL/6N mice. *Nutr. Diabetes* 7, e261 (2017).

16. Guo, J., Jou, W., Gavrilova, O. & Hall, K. D. Persistent diet-induced obesity in male C57BL/6 mice resulting from temporary obesigenic diets. *PLoS ONE* 4, e5370 (2009).

17. Klok, M. D., Jakobsdottir, S. & Drent, M. L. The role of leptin and ghrelin in the regulation of food intake and body weight in humans: a review. *Obes. Rev.* 8, 21-34 (2007).

18. Ioannou, G. N., Weiss, N. S., Boyko, E. J., Mozaffarian, D. & Lee, S. P. Elevated serum alanine aminotransferase activity and calculated risk of coronary heart disease in the United States. *Hepatology* 43, 1145-1151 (2006).

19. Kleiner, D. E. et al. Design and validation of a histological scoring system for nonalcoholic fatty liver disease. *Hepatology* 41, 1313-1321 (2005).

20. Fontana, L. et al. Aging promotes the development of diet-induced murine steatohepatitis but not steatosis. *Hepatology* 57, 995-1004 (2013).

21. Goedecke, J. H. et al. Determinants of the variability in respiratory exchange ratio at rest and during exercise in trained athletes. *Am. J. Physiol. Endocrinol. Metab.* 279, 1325-1334 (2000).

22. Shiojima, I. Disruption of coordinated cardiac hypertrophy and angiogenesis contributes to the

transition to heart failure. *J. Clin. Invest.* 115, 2108-2118 (2005).

23. Xu, X. et al. Age-related impairment of vascular structure and functions. *Aging Dis.* 8, 590-610 (2017).

24. Lakatta, E. G. Arterial and cardiac aging: major shareholders in cardiovascular disease enterprises: part III: cellular and molecular clues to heart and arterial aging. *Circulation* 107, 490-497 (2003).

25. Horn, M. A. & Trafford, A. W. Aging and the cardiac collagen matrix: novel mediators of fibrotic remodelling. *J. Mol. Cell. Cardiol.* 93, 175-185 (2016).

26. Nadruz, W. Myocardial remodeling in hypertension. *J. Hum. Hypertens.* 29, 1-6 (2015).

27. Houser, S. R. et al. Animal models of heart failure. *Circ. Res.* 111, 131-150 (2012).

28. Marwick, T. H. Stress echocardiography. In *Echocardiography* (eds Nihoyannopoulos, P. & Kisslo, J.) 491-519 (Springer, 2018).

29. Vallet, B., Dupuis, B. & Chopin, C. [Dobutamine: mechanisms of action and use in acute cardiovascular pathology]. *Ann. Cardiol. Angeiol.* 40, 397-402 (1991).

30. Pellikka, P. A. et al. Guidelines for performance, interpretation, and application of stress echocardiography in ischemic heart disease: from the American Society of Echocardiography. *J. Am. Soc. Echocardiogr.* 33, 1-41 (2020).

31. Zhang, Y. et al. Obesity-induced oxidative stress, accelerated functional decline with age and increased mortality in mice. *Arch. Biochem. Biophys.* 576, 39-48 (2015).

32. Leontieva, O. V., Paszkiewicz, G. M. & Blagosklonny, M. V. Weekly administration of rapamycin improves survival and biomarkers in obese male mice on high-fat diet. *Aging Cell* 13, 616-622 (2014).

33. Aires, V. et al. Healthy adiposity and extended lifespan in obese mice fed a diet supplemented with a polyphenol-rich plant extract. *Sci. Rep.* 9, 9116-9134 (2019).

34. Zhu, B. et al. Alogliptin improves survival and health of mice on a high-fat diet. *Aging Cell* 18, e12883 (2019).

35. Brandhorst, S. & Longo, V. D. Dietary restrictions and nutrition in the prevention and treatment of cardiovascular disease. *Circ. Res.* 124, 952-965 (2019).

36. Fanti, M., Mishra, A., Longo, V. D. & Brandhorst, S. Time-restricted eating, intermittent fasting, and fasting-mimicking diets in weight loss. *Curr. Obes. Rep.* 10, 70-80 (2021).

37. Newman, J. C. et al. Ketogenic diet reduces midlife mortality and improves memory in aging mice. *Cell Metab.* 26, 547-557 (2017).

38. Rusli, F. et al. Intermittent calorie restriction largely counteracts the adverse health effects of a moderate-fat diet in aging C57BL/6J mice. *Mol. Nutr. Food Res.* 61, 1600677 (2017).

39. Stamler, J. et al. Relationship of baseline serum cholesterol levels in 3 large cohorts of younger men to long-term coronary, cardiovascular, and all-cause mortality and to longevity. *JAMA* 284, 311-318 (2000).

40. Sedej, S. Ketone bodies to the rescue for an aging heart? *Cardiovasc. Res.* 114, e1-e2 (2018).

41. Veech, R. L. et al. Ketone bodies mimic the life span extending properties of caloric restriction. *IUBMB Life* 69, 305-314 (2017).

42. Greenway, F. L. Physiological adaptations to weight loss and factors favouring weight regain. *Int. J. Obes.* **39**, 1188-1196 (2015).

43. Graham, B., Chang, S., Lin, D., Yakubu, F. & Hill, J. O. Effect of weight cycling on susceptibility to dietary obesity. *Am. J. Physiol.* 259, R1096-R1102 (1990).

44. Simonds, S. E., Pryor, J. T. & Cowley, M. A. Repeated weight cycling in obese mice causes increased appetite and glucose intolerance. *Physiol. Behav.* 194, 184-190 (2018).

45. O'Connor, K. L. et al. Altered appetite-mediating hormone concentrations precede compensatory overeating after severe, short-term energy deprivation in healthy adults. *J. Nutr.* 146, 209-217 (2016).

46. Coutinho, S. R. et al. Compensatory mechanisms activated with intermittent energy restriction: a randomized control trial. *Clin. Nutr.* 37, 815-823 (2018).

47. Kondo, M. et al. Caloric restriction stimulates revascularization in response to ischemia via adiponectin-mediated activation of endothelial nitric-oxide synthase. *J. Biol. Chem.* 284, 1718-1724 (2009).

48. Claudio, deL. et al. Long-term caloric restriction improves cardiac function, remodeling, adrenergic responsiveness, and sympathetic innervation in a model of postischemic heart failure. *Circ. Heart Fail.* 11, e004153 (2018).

49. Ahmet, I., Tae, H.-J., de Cabo, R., Lakatta, E. G. & Talan, M. I. Effects of calorie restriction on cardioprotection and cardiovascular health. *J. Mol. Cell. Cardiol.* 51, 263-271 (2011).

50. Kim, S. S. et al. Whole-transcriptome analysis of mouse adipose tissue in response to short-term caloric restriction. *Mol. Genet. Genomics* 291, 831-847 (2016).

51. Nisoli, E. et al. Calorie restriction promotes mitochondrial biogenesis by inducing the expression of eNOS. *Science* 310, 314-317 (2005).

52. Pardo, R. et al. Calorie restriction prevents diet-induced insulin resistance independently of PGC-1-driven mitochondrial biogenesis in white adipose tissue. *FASEB J.* 33, 2343-2358 (2018).

53. Kusminski, C. M. & Scherer, P. E. Mitochondrial dysfunction in white adipose tissue. *Trends Endocrinol. Metab.* 23, 435-443 (2012).

54. Katic, M. et al. Mitochondrial gene expression and increased oxidative metabolism: role in increased lifespan of fat-specific insulin receptor knock-out mice. *Aging Cell* 6, 827-839 (2007).

55. Edgar, R., Domrachev, M. & Lash, A. E. Gene Expression Omnibus: NCBI gene expression and hybridization array data repository. *Nucleic Acids Res.* 30, 207-210 (2002).

56. Vinué, À. & Gonzalez-Navarro, H. Glucose and insulin tolerance tests in the mouse. In *Methods in Mouse Atherosclerosis* (eds Andrés, V. & Dorado, B.) 247-254 (Springer, 2015).

57. Lancellotti, P. et al. The clinical use of stress echocardiography in non-ischaemic heart disease:

recommendations from the European Association of Cardiovascular Imaging and the American Society of Echocardiography. *Eur. Heart J. Cardiovasc. Imaging* 17, 1191-1229 (2016).

58. Barone, R. et al. Skeletal muscle heat shock protein 60 increases after endurance training and induces peroxisome proliferator-activated receptor γ coactivator 1 al expression. *Sci. Rep.* 6, 19781 (2016).

59. Dobin, A. et al. STAR: ultrafast universal RNA-seq aligner. *Bioinformatics* 29, 15-21 (2013).

60. Ritchie, M. E. et al. limma powers differential expression analyses for RNA-sequencing and microarray studies. *Nucleic Acids Res.* 43, e47 (2015).

61. Robinson, M. D. & Oshlack, A. A scaling normalization method for differential expression analysis of RNA-seq data. *Genome Biol.* 11, R25 (2010).

62. Law, C. W., Chen, Y., Shi, W. & Smyth, G. voom: precision weights unlock linear model analysis tools for RNA-seq read counts. *Genome Biol.* 15, R29 (2014).

63. Chen, H. & Boutros, P. C. VennDiagram: a package for the generation of highly-customizable Venn and Euler diagrams in R. *BMC Bioinformatics* 12, 35 (2011).

64. Chen, E. Y. et al. Enrichr: interactive and collaborative HTML5 gene list enrichment analysis tool. *BMC Bioinformatics* 14, 128 (2013).

65. Kuleshov, M. V. et al. Enrichr: a comprehensive gene set enrichment analysis web server 2016 update. *Nucleic Acids Res. 44,* W90-W97 (2016).

66. Walter, W., Sanchez-Cabo, F & Ricote, M. GOplot: an R package for visually combining expression data with functional analysis. *Bioinformatics 31*, 2912-2914 (2015).

Acknowledgements

Funding was provided by the USC Edna Jones chair fund and NIH P01 AG055369-01 to V.D.L. This work was also funded, in part, by the Intramural Research Program of the National Institutes of Health/NIA. We acknowledge support from the USC Molecular Imaging Center and the USC Leonard Davis School Aging Murine Phenotyping Core Facility. A. Mouton was supported by a QCB Collaboratory Postdoctoral Fellowship (UCLA). We used computational and storage services associated with the Hoffman2 Shared Cluster provided by the UCLA Institute for Digital Research and Education's Research Technology Group.

Author contributions

V.D.L. conceived the original idea and supervised the project. V.D.L., M.W., T.E.M. and H.M. designed mouse experiments. H.M., S.B. and S.D.B. collected tissue. G.N. prepared the mouse FMD. M.V., F.R. and R.B. processed and performed immunohistochemistry and quantitative analysis. H.M. performed alanine transaminase, ketone body and serum cholesterol quantification. A. Mishra performed quantification of blood glucose, triglycerides, leptin and ghrelin and the GTT and ITT. N.G. designed and analysed the metabolic cage experiment. N.G. and G.N. performed the metabolic cage experiment. H.M. and S.R.K. performed the stress echocardiography experiment;

S.R.K. analysed echocardiography data. V.D.L., N.G. and M.P. designed the RNA-seq experiment.

A. Mishra, A. Mouton and M.L. analysed RNA-seq data and made figures. T.E.M., M.W. and P.S.C. were involved in study design. A. Mishra prepared the figures and wrote the initial draft. A. Mishra and V.D.L. revised the manuscript with input from all authors. R.d.C. and M.B. contributed to interpretation, review and final editing.

Competing interests

V.D.L. has equity interest in L-Nutra, which develops and sells medical food for the prevention and treatment of diseases. V.D.L. has committed all his equity in the company to charitable organizations. All other authors declare no competing interests.

Additional information

Extended data is available for this paper at https://doi.org/10.1038/s42255-021-00469-6.

Supplementary information The online version contains supplementary material available at https://doi.org/10.1038/s42255-021-00469-6.

Correspondence and requests for materials should be addressed to Valter D. Longo.

Peer review information *Nature Metabolism* thanks Leonie Heilbronn, Satchidananda Panda and William Sessa for their contribution to the peer review of this work. Primary handling editor: Christoph Schmitt.

Extended Data Fig. 1 | Project Outline and serum ALT measurement. *Extended Data Fig. 1, related to Fig. 1. Project Outline and serum ALT measurement. a) Schematic representation of the outline of the project. b) Timeline for procedures and functional tests. c) Serum ALT activity to assay liver function at the end of 10 cycles, fourteen days after refeeding. One-way ANOVA, p = 0.1625 ns. Control (n = 6), HFCD (n = 3), HFCD + FMD (n = 4). Data are shown as the mean ± SEM.*

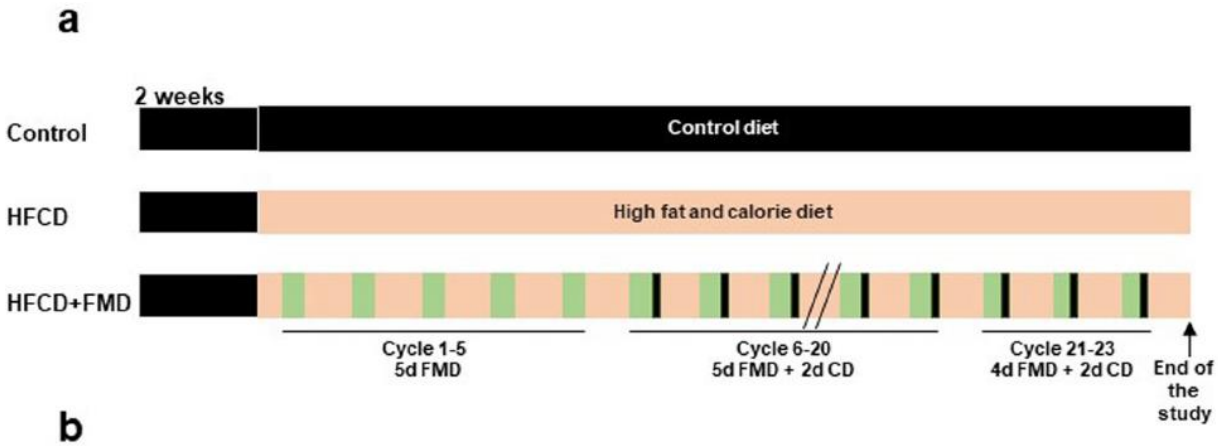

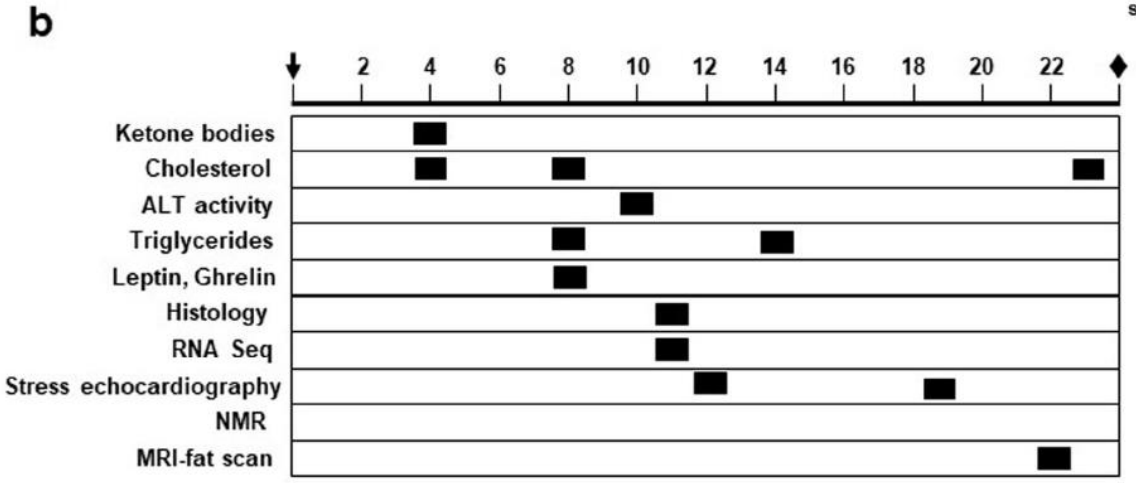

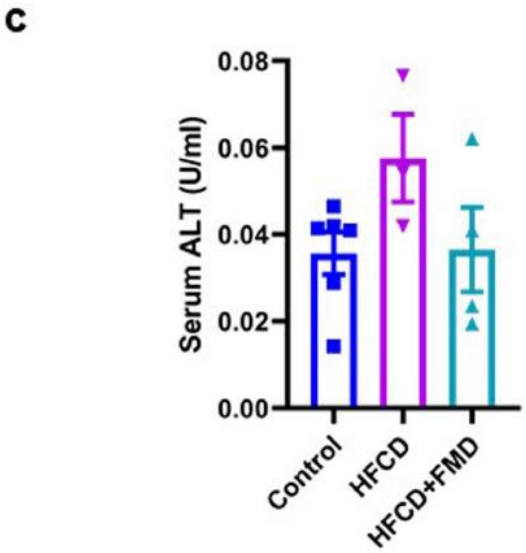

Extended Data Fig. 2 | Liver weight and histological assessment after 11 cycles of FMD. *Extended Data Fig. 2 related to Fig. 2. Liver weight and histological assessment after 11 cycles of FMD. a) Liver weight. One-way ANOVA, p = 0.0010***. Tukey's multiple comparisons tests: Control vs. HFCD, p = 0.0399 *; Control vs. HFCD + FMD, p = 0.0007 ***; HFCD vs. HFCD + FMD, p = 0.2549 ns. Control (n = 6), HFCD (n = 4), HFCD + FMD (n = 6). Data are shown as the mean ± SEM. b) Liver weight to body weight ratio. One-way ANOVA, p = 0.0061. Tukey's multiple comparisons tests: Control vs. HFCD, p = 0.0404 *; Control vs. HFCD + FMD, p = 0.4297 ns; HFCD vs. HFCD + FMD, p = 0.0048 **. Control (n = 6), HFCD (n = 4), HFCD + FMD (n = 6). Data are shown as the mean ± SEM. c) Liver histological score. One-way ANOVA, p = 0.2314 ns. Control (n = 12), HFCD (n = 11), HFCD + FMD (n = 8). Data are shown as the mean ± SEM. d) Steatosis score. One-way ANOVA, p = 0.4541 ns. Control (n = 12), HFCD (n = 11), HFCD + FMD (n = 8). Data are shown as the mean ± SEM.*

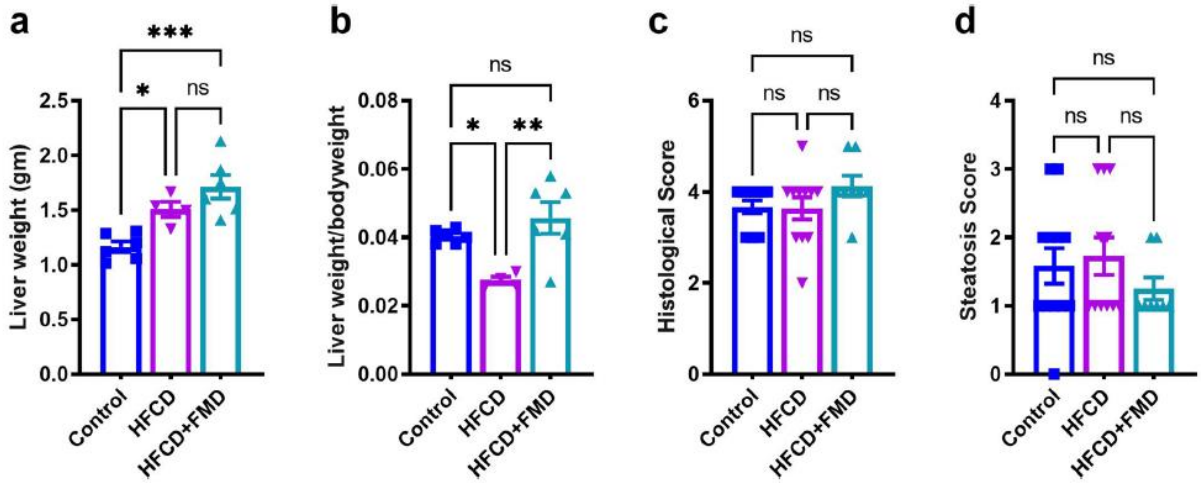

Extended Data Fig. 3 | Collagen I and collagen III staining and quantification in aorta. *Extended Data Fig. 3 related to Fig. 4. Collagen I and collagen III staining and quantification in aorta. a) Representative image of Collagen I immunostaining in aorta. Collagen I (green), DAPI (blue). b) Immunofluorescence quantification of Collagen I expression. One-way ANOVA, p = 0.2549 ns. c) Representative image of Collagen III immunostaining in aorta. Collagen III (green), DAPI (blue). d) Immunofluorescence quantification of Collagen III expression. One-way ANOVA, p = 0.0285 *. Tukey's multiple comparisons tests; Control vs. HFCD, p = 0.0320 *, Control vs. HFCD + FMD, p = 0.8694 ns, HFCD vs. HFCD + FMD, p = 0.0830 ns. Data are shown as mean ± SEM, n = 6 mice per group.*

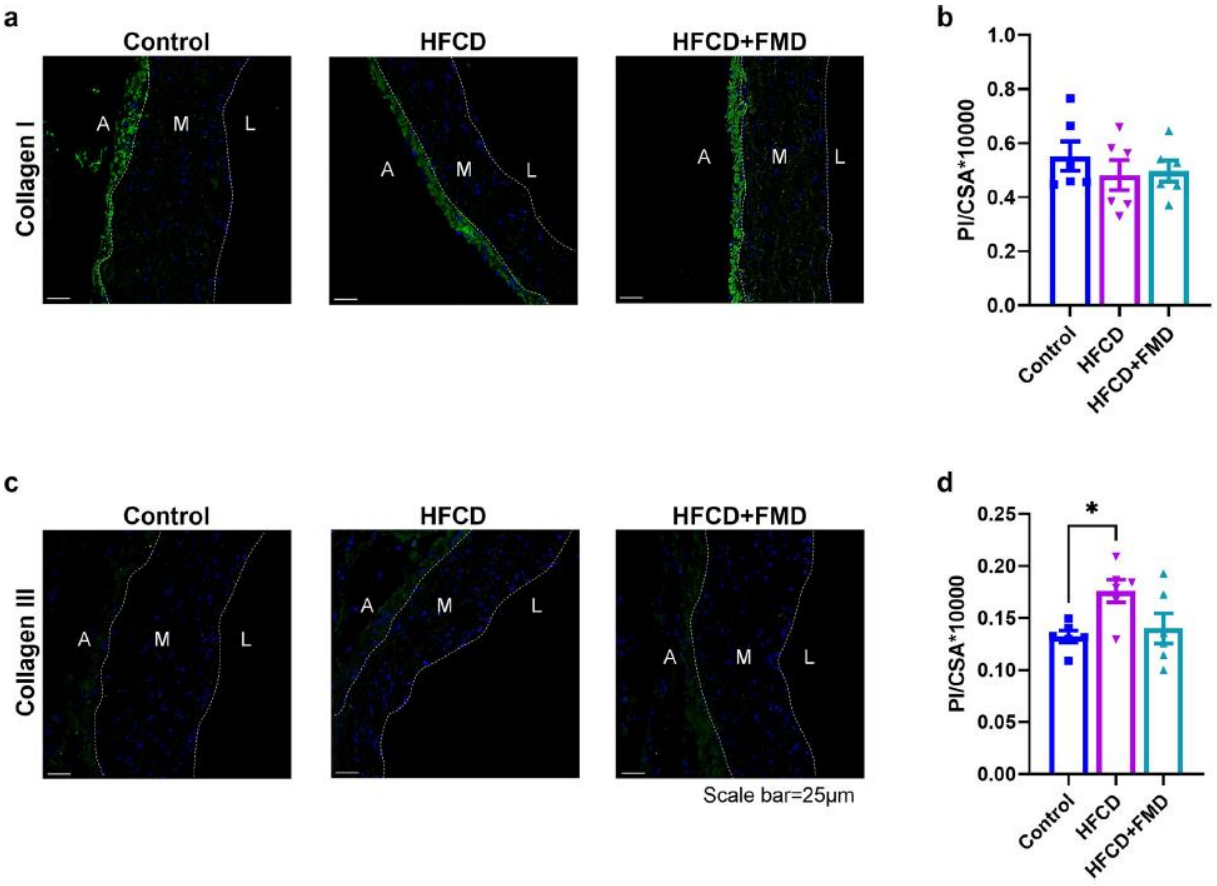

Extended Data Fig. 4 | Stress-echocardiography analysis during the 12th cycle of FMD. *Extended Data Fig. 4 related to Fig. 4. Stress-echocardiography analysis during the 12th cycle of FMD. a) Recovery time from the stress echocardiography measured in min (time taken to return to normal echo). One-way ANOVA, p = 0.4641 ns. b) End Diastolic Volume (EDV). One-way ANOVA, p = 0.8580 ns. c) Left ventricle internal diameter-diastolic (LVID-d). One-way ANOVA, p = 0.8683 ns. d) Interventricular septal thickness-diastolic. One-way ANOVA, p = 0.7956 ns. e) Left ventricle posterior wall thickness-diastolic (LVPW-d). One-way ANOVA, p = 0.4899 ns. f) Left ventricle mass (LV mass). One-way ANOVA, p = 0.9459 ns. Data are shown as mean ± SEM, n = 6 mice per group.*

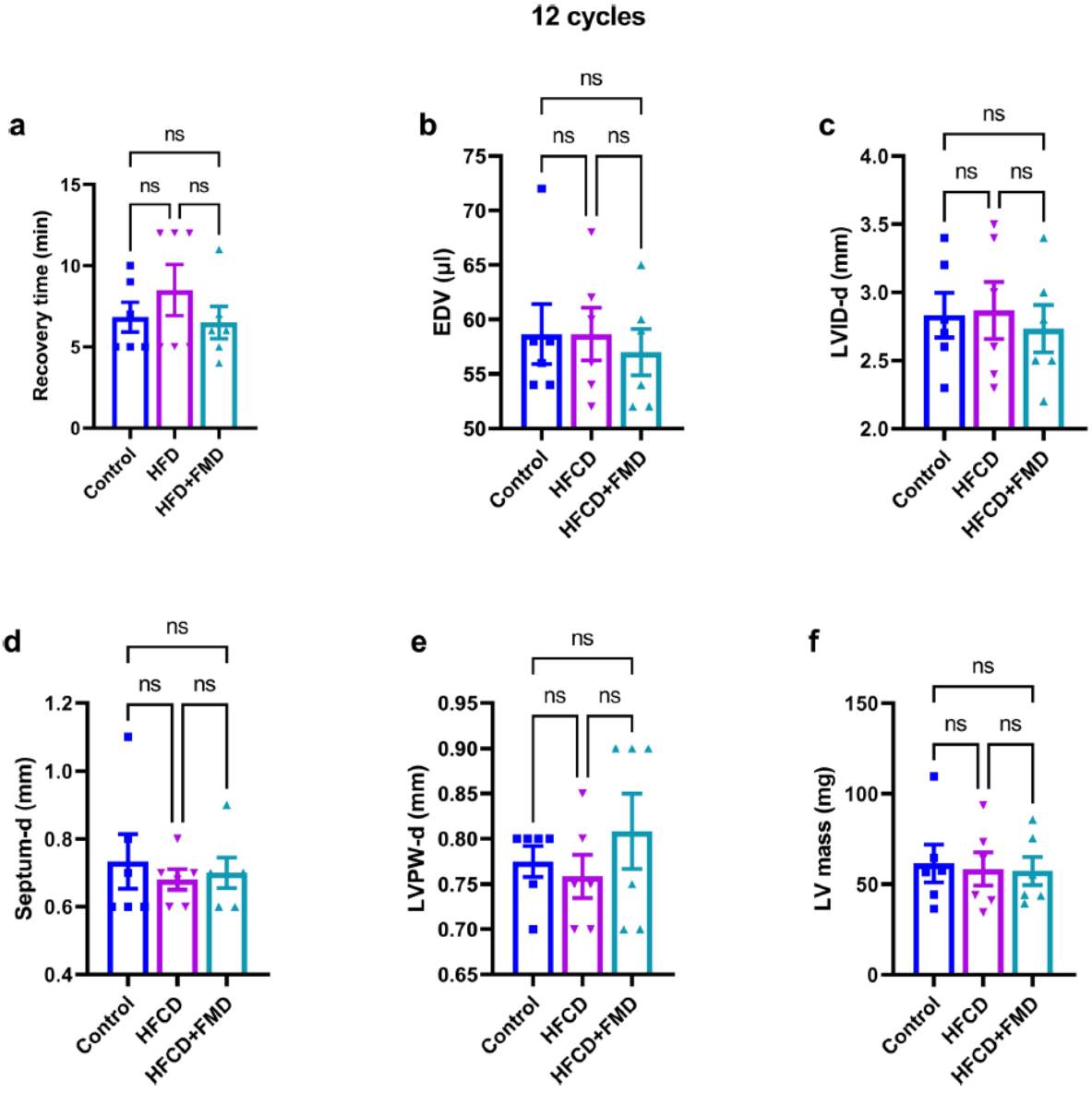

Extended Data Fig. 5 | KEGG and Wikipathways analyses of differentially expressed genes. *Extended Data Fig. 5 related to Fig. 5. KEGG and Wikipathways analyses of differentially expressed genes. KEGG and WikiPathways analyses of differentially expressed genes (DEGs) present in the heart (a) and visceral adipose tissue (b) in Control vs. HFCD (BD) pairwise comparison but absent in Control vs. HFCD + FMD (BC). Adjusted p-value < 0.05.*

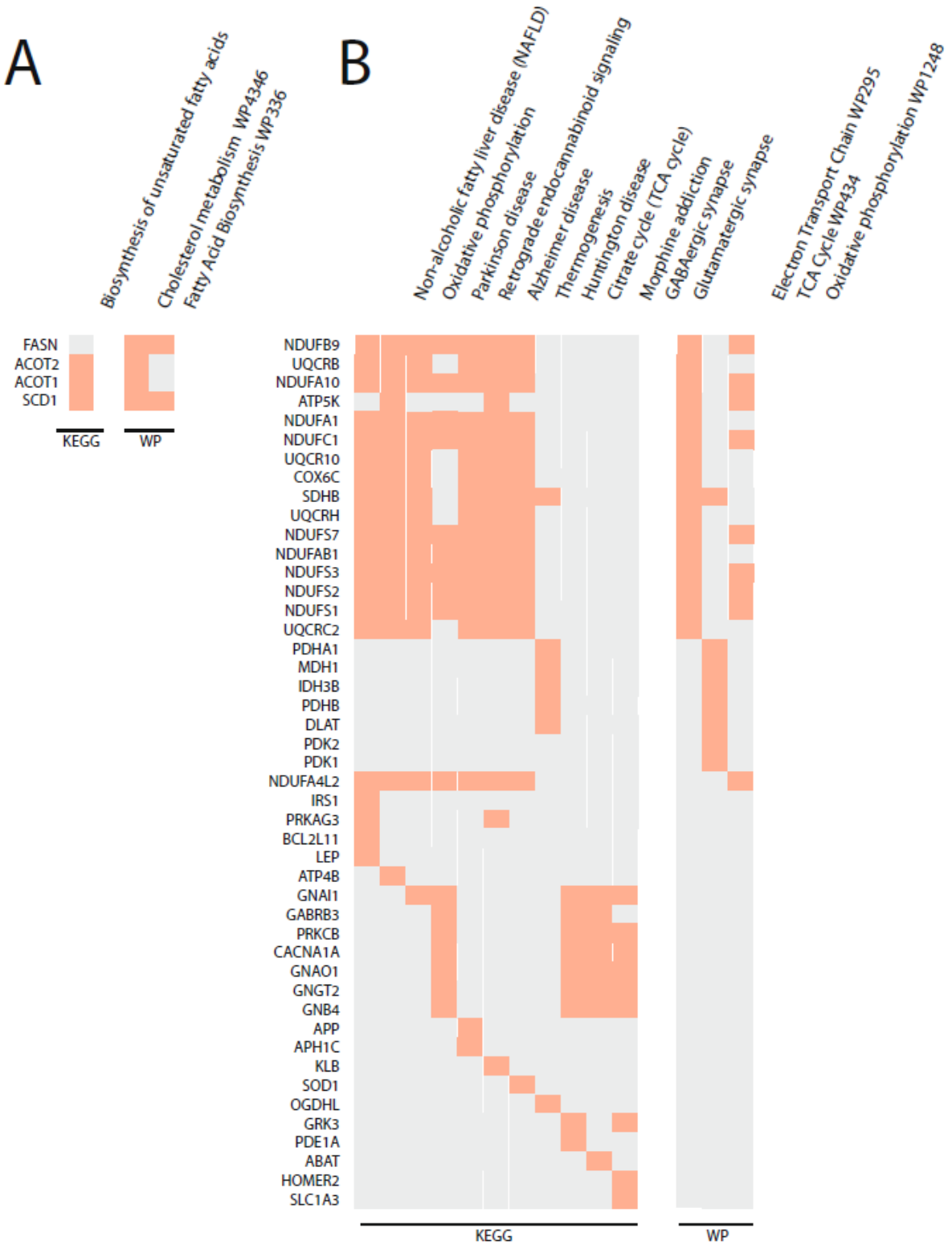

Extended Data Fig. 6 | Heatmaps representing gene expression levels of the genes identified by KEGG and Wikipathways analyses. *Extended Data*

Fig. 6 related to Fig. 5. Heatmaps representing gene expression levels of the genes identified by KEGG and Wikipathways analyses. a,b) Heatmaps representing the levels of DEGs present in the heart (a) and adipose visceral adipose tissue (b, c) in the Control vs. HFCD (BD) pairwise comparison but absent in Control vs. HFCD + FMD (BC). DEG enrichment in select pathways as identified by KEGG and WikiPathways analyses. Adjusted p-value < 0.05 & abs(logFC) >1.0 (fold change>2).